STRENGTHENING OF A Cu-9Ni-6Sn ALLOY BY THERMOMECHANICAL TREATMENT

By
S. DEVARAJ

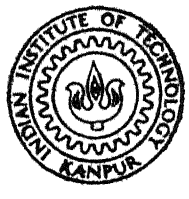

DEPARTMENT OF METALLURGICAL ENGINEERING
INDIAN INSTITUTE OF TECHNOLOGY KANPUR

DECEMBER 1979

STRENGTHENING OF A Cu-9Ni-6Sn ALLOY BY THERMOMECHANICAL TREATMENT

A Thesis Submitted
in Partial Fulfilment of the Requirements
for the Degree of
MASTER OF TECHNOLOGY

By
S. DEVARAJ

to the
DEPARTMENT OF METALLURGICAL ENGINEERING
INDIAN INSTITUTE OF TECHNOLOGY KANPUR
DECEMBER 1979

CERTIFICATE

This is to certify that the present work 'STRENGTHENING OF A Cu-9Ni-6Sn ALLOY BY THERMOMECHANICAL TREATMENT' has been carried out under my supervision and has not been submitted elsewhere for a degree.

Date: December 31, 1979

[R.K. Ray]
Assistant Professor
Department of Metallurgical Engineering
Indian Institute of Technology,
Kanpur-208016, India

ACKNOWLEDGEMENTS

The author wishes to express his gratitude to Dr. R.K. Ray for his invaluable guidance and constant encouragement throughout this work. He is thankful to Dr.A. Ghosh for providing laboratory facilities.

The author is grateful to his colleague Mr. S. Chandranarayanan for his valuable and unstinted assistance during this work.

The author is thankful to Mr. Samar Das for his valuable help and cooperation. He also wishes to thank Mr. A. Sharma and Mr. Ram Ashis Rai for their help during this work.

The author is thankful to Mr. B.S. Pandey for his excellent typing.

Author

CONTENTS

CHAPTER

SYNOPSIS

The transformations occurring in a Cu-9Ni-6Sn alloy have been studied by optical microscopy, electron microscopy and x-ray diffraction. The sequence of the transformation in the alloy was found to be solid solution ----> spinodal decomposition ----> ordering ----> discontinuous precipitates. This sequence was maintained in both non prior cold worked and prior cold-worked alloy. The mechanical properties of the alloy at different stages of heat treatment have been obtained by tensile testing on an instron testing machine. The maximum yield and tensile strength was obtained in the alloy by cold rolling and aging for 10 minutes at 350°C. The strengthening has been found to be due to the modulated structure obtained due to spinodal decomposition.

CHAPTER 1

INTRODUCTION

Thermo mechanical treatment (TMT) is a combination of thermal and mechanical processes which modifies the structural transformation to give a better combination of strength and ductility. It consists of the application of plastic deformation either before, during or after a phase transformation. TMT is very widely used in the case of steel. However, this has not gained much importance for non ferrous alloys. Hart [1] and co-workers have done some pioneering work on the TMT of copper base alloys in the early seventies. They studied the strengthening by TMT on Phosphor bronze, Nickel silver, Copper-Beryllium and Copper-Nickel-Tin alloys and their results were very encouraging. Plewes [2] has done further work on the Cu-9Ni-6Sn alloy and has obtained unique combinations of yield stress and ductility.

The mechanical properties are undoubtedly a function of the relevant microstructures developed in these alloys by suitable TMT. The existing literature in case of Cu-Ni-Sn alloys shows that there has been some controversy [3] regarding the type of structures produced by conventional and TMT methods. Hence there is ample scope for doing further research in this area and throw some new light.

It was with these ideas that the present work was started. Using a number of research techniques like transmission electron microscopy, x-ray diffraction etc., a systematic study has been made to find out the structural features produced in a nominal Cu-9Ni-6Sn alloy consequent upon TMT and after conventional heat treatment. Further these microstructural features have been correlated with the corresponding mechanical property values and attempts have been made, on this basis, to suggest suitable TMT schedules for the realisation of the optimum properties in this alloy.

CHAPTER 2

LITERATURE REVIEW

2.1 Age Hardening Copper Base Alloys:

2.1.1 Phase Diagrams:

The important age hardening copper base alloys are 1. Copper-Beryllium 2. Copper-Titanium and 3. Copper-Nickel-Tin. The phase diagrams of these alloys are shown in Figures 2.1 to 2.3.

2.1.2 Mechanical Properties:

Copper-Beryllium: The alloy of commercial importance in this system is the copper- 2 per cent Beryllium alloy. The mechanical properties [4] of this alloy are shown in Table 2.1.

Copper-Titanium: The important alloy in this system is Copper- 4.3 per cent Titanium which exhibits the best mechanical properties [5]. The mechanical properties of this alloy are shown in Table 2.2.

Copper-Nickel-Tin: Moderate levels of Nickel have been added to a variety of bronzes for a number of years to improve fluidity characteristics, refine grain size and increase hardness in the as-cast condition. Larger additions were known to significantly increase the hardness but the ductility was severely impaired.

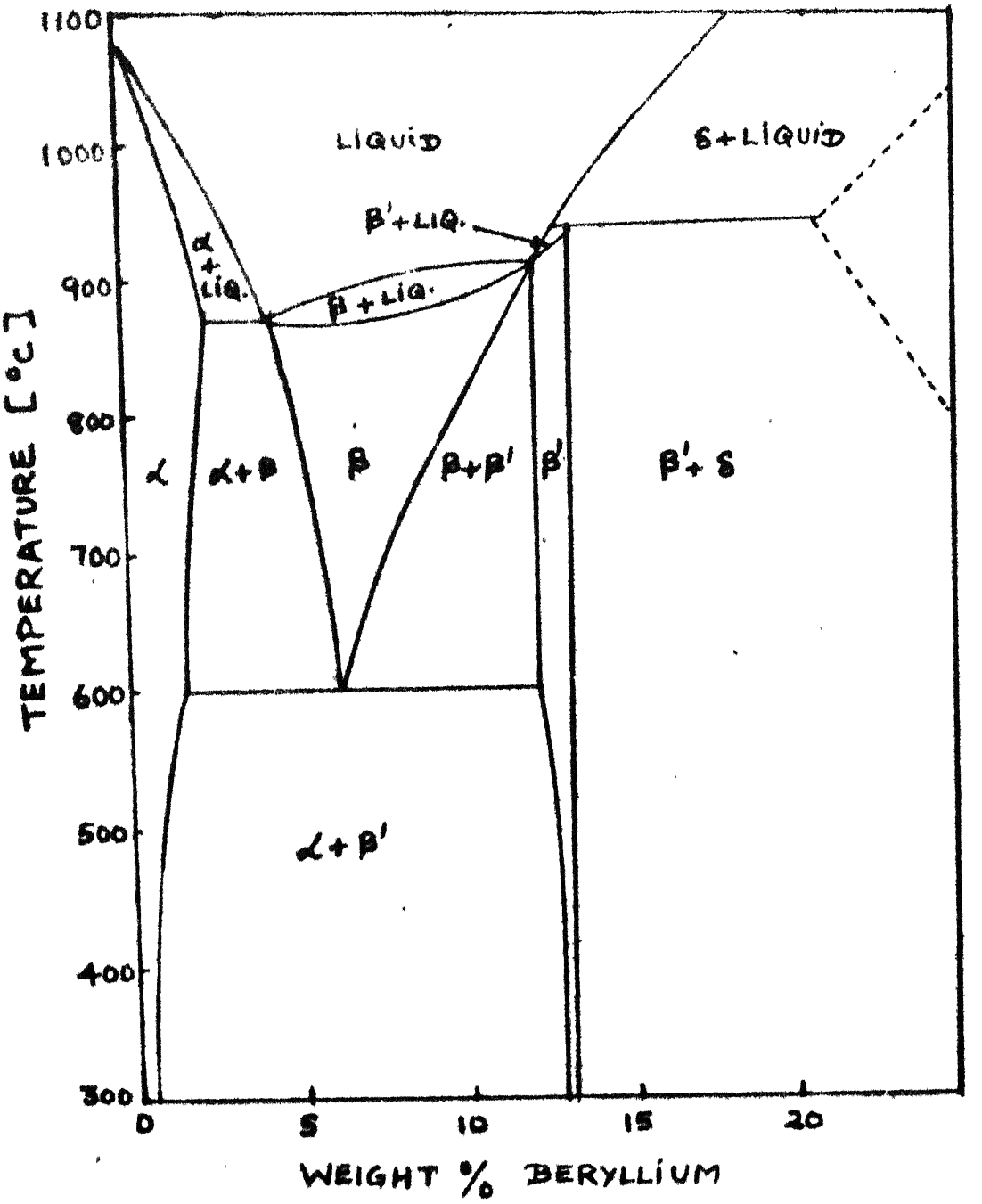

Fig. 2.1 - Copper-Berylliumequilibrium diagram.

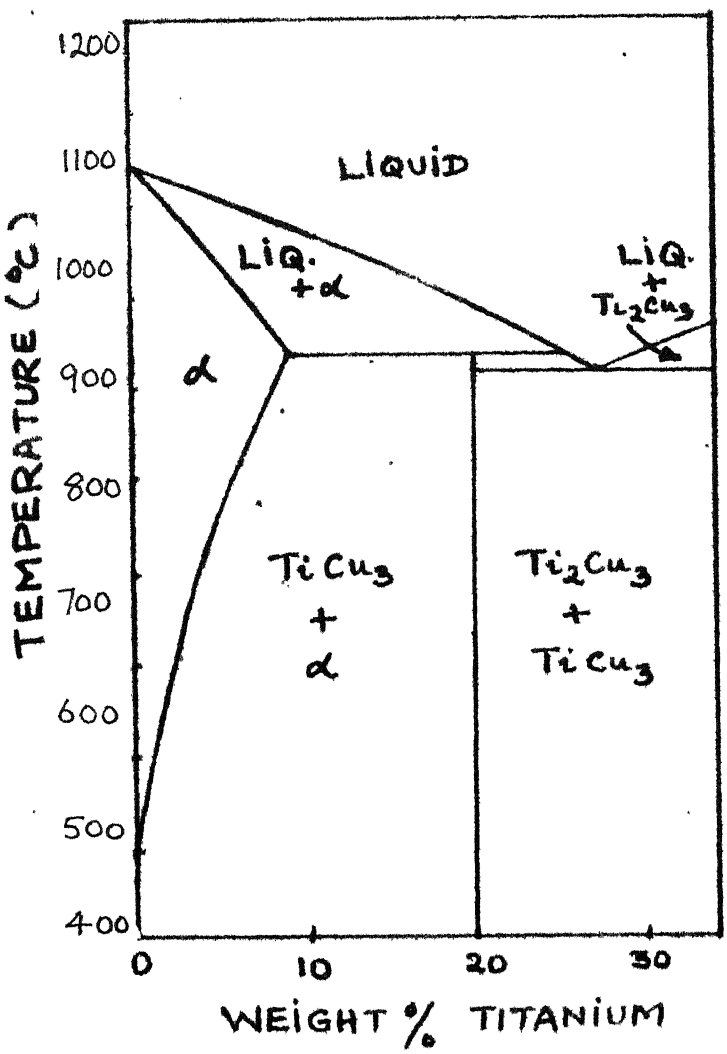

Fig. 2.2 - Copper - Titanium equilibrium diagram.

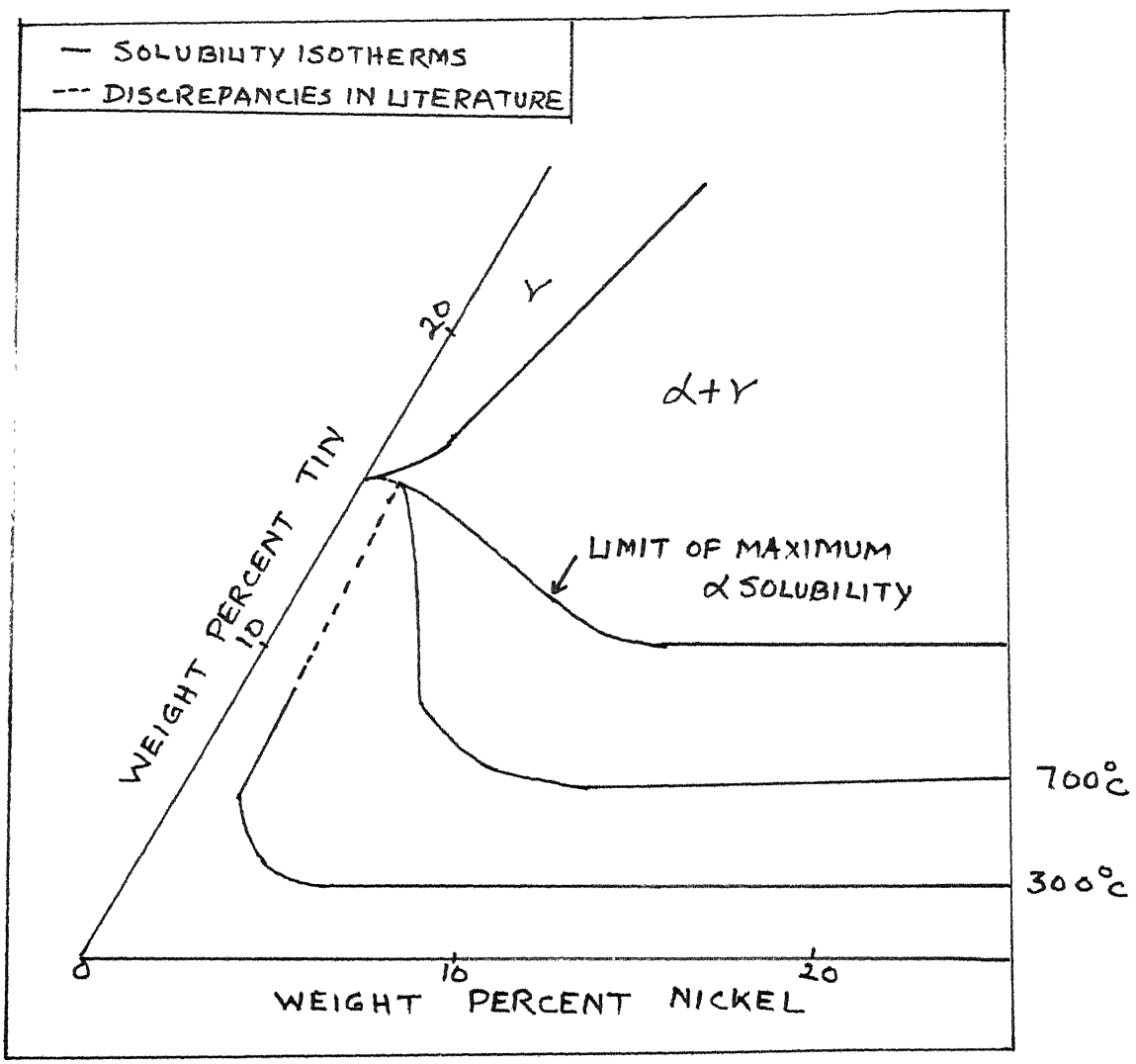
— SOLUBILITY ISOTHERMS
--- DISCREPANCIES IN LITERATURE
20
γ
α+γ
WEIGHT PERCENT TIN
10
LIMIT OF MAXIMUM
α SOLUBILITY
700°C
300°C
0
10
20
WEIGHT PERCENT NICKEL

TABLE 2.1: MECHANICAL PROPERTIES OF THE COPPER - 2 PER CENT BERYLLIUM ALLOY

Condition of the alloy	Ultimate Tensile strength in Ksi	Yield strength in Ksi	Percentage Elongation
As annealed	60 to 80	20 to 30	35 to 50
Precipitation Hardened	165 to 185	150 to 170	1 to 5

TABLE 2.2: MECHANICAL PROPERTIES OF THE COPPER - 4.3 PER CENT TITANIUM ALLOY

Condition of the alloy	Ultimate tensile strength in Ksi	Percentage Elongation
As annealed	75	22.0
Cold rolled (85 percent)	175	1.8
Cold rolled and precipitation hardened	205	1.0

TABLE 2.3: MECHANICAL PROPERTIES OF THE Cu-9Ni-6Sn ALLOY

Condition of the alloy	Yield strength (.01 per cent offset) in Ksi	Percentage reduction in area
As annealed	15	82
Annealed and hardened	88	10
Cold rolled (99 per cent) and hardened	174	55

Leo [6] investigated the isothermal aging response in a Cu-6Ni-6Sn alloy. He found that large changes in hardness could be obtained by aging at temperatures less than 400°C. Above this temperature the hardening response was slight. Below 400°C, TEM revealed a very finely dispersed continuous transformation which could not be identified. This has been identified by Schwartz [7] et al. as a product of spinodal decomposition. They have found that spinodal decomposition occurs on aging 300 to 350°C below the equilibrium phase boundary. They have shown that this leads to strengthening in the Cu-9Ni-6Sn alloy.

Plewes [2] has shown that the Cu-9Ni-6Sn may be thermo-mechanically processed to exhibit a 0.01 per cent offset yield strength of 174 Ksi together with a 55 per cent reduction of area on fracture. They have obtained a significant increase in the yield strength value of the cold worked state after aging for short time intervals at 350°C. They have explained that this increase was due to the modulated structure obtained due to spinodal decomposition.

However, Holmi [3] et al, who made a study of this alloy by x-ray diffraction, have contradicted this. They have explained that the heavily deformed state of the lattice would prevent spinodal decomposition. The inhomogeneous dislocation network generated by plastic deformation would form nucleation centers for precipitation. In these regions

the diffusion would be controlled by the strain gradient rather than by the concentration gradient. The uphill diffusion would thus be hindered. They concluded that the apparent periodicity of the structure observed by Plewes [2] in electron micrographs could be caused by more or less periodic arrangement of the nucleation centers.

The mechanical properties [2] of the Cu-9Ni-6Sn alloy are shown in Table 2.3.

2.1.3 Microstructural Aspects:

Copper-Beryllium: The first detailed electron microscopic study of the Cu-Be system was done by Tanner [8]. He studied only the initial stages of the transformation. The as quenched alloy showed a uniform mottling in all grains and this was in stronger contrast at extinction points. The diffraction patterns revealed diffuse scattering at each spot. On aging for 30 minutes at 200°C a unique striated microstructure was developed. The diffraction patterns showed distinct 100 and 110 relrods. On aging upto 14 hours there was a progressive increase in the intensity of the relrods in diffraction patterns and the contrast of the striations in the microstructure was improved. He found by stereographic analysis that the striations were parallel to the 110 traces. The diffraction effects indicated that the initial reaction product was a thin disc shaped precipitate or G.P. zone

parallel to the cube planes of the matrix. Tanner concluded that the striated structure was a strain contrast effect due to the coherency of the G.P. zones.

G. Thomas [9] and Yamamoto [10] et al. have reported similar structures. In their study the as quenched microstructure did not show any dislocation configuration resulting from vacancy condensation which was expected in age hardenable alloys. They explained that this was because most of the quenched in vacancies were held in supersaturation and were probably associated with Beryllium atoms. The aged alloy developed the unique striated microstructure which is also known as 'tweed' structure. Yamamoto [10] observed that the striations did not possess such a distinct image such as dislocations or stacking faults but were rather a basket weave of light and dark contrast. The striations were found to have a high density and were distributed uniformly throughout the microstructure. On further aging at higher temperatures the γ' precipitates with a B.C.T. structure were obtained. This was followed by the equilibrium γ precipitate with a B.C.C. unit cell at still higher aging temperatures.

Copper-Titanium: Cornie [11] et al. made the first detailed electron microscope study of the copper-Titanium system. They studied both the Cu-3 per cent Ti and Cu-4 per cent Ti alloys. The electron micrographs of the as

quenched alloy showed a modulated structure. The modulated structure was characterised by finely distributed contrast striations along the traces of the $\{100\}$ matrix planes or rod like clusters along the $\langle 100 \rangle$ directions. Electron diffraction patterns of the as-quenched specimens showed sidebands along $\langle 100 \rangle$. The wavelength of the modulated structure as calculated by the Daniel and Lipson [12] relationship was 50 to 60 Å in the as quenched specimen. On aging at 400°C cluster growth occurred and the wavelength of the periodic structure gradually increased. The electron diffraction patterns showed that as aging progressed the sidebands moved towards the matrix reflection and eventually became indistinguishable from the matrix spot. After aging the Cu-4 per cent Ti alloy for 20 hours at 400°C diffuse streaking along the $\langle 100 \rangle$ directions was noticed. The diffraction pattern showed splitting of the diffraction spots along the $\langle 100 \rangle$ directions. Cornie [11] et al. have explained that this splitting was associated with the formation of the metastable tetragonal β' phase. They also explained that the appearance of the β' phase was not associated with a breakdown of coherency and the generation of interfacial dislocations since dislocation networks could not be observed at interfaces. However, the micrographs showed δ fringes at this stage which were typical of coherent boundaries arising from Δs and Δg mismatch

in reciprocal space across the coherent interfaces. The maximum strength values were associated with the formation of the β' phase in the Cu-Ti alloys. On further aging the equilibrium Cu_3Ti phase was formed as a discontinuous precipitate. Overaging was associated with the formation of the equilibrium phase.

Dutkierwick [13] and Dutta [14] et al., who have made recent studies, have reported similar microstructures. In addition they found weak superlattice reflections in the diffraction patterns at the early stages of aging. The superlattice reflections were found to become sharper and more intense during prolonged aging.

Dutkiewicz [13] have studied the microstructure of deformed and aged alloys in addition to the annealed and aged alloys. The as deformed (70 per cent) alloy showed elongated sub grains within the grains and deformation bands. On aging at 400°C no ordering was observed while annealed and aged 400°C alloy showed ordering. They concluded that the effect of deformation in depressing the ordering process might result from heterogeneous precipitation on crystal defects which decreases the titanium content in the solid solution. The deformation was also found to influence the discontinuous precipitation. On aging at 400°C the discontinuous precipitates nucleate at the grain boundary, subgrain boundary and deformation bands.

Laughlin and Cahn [15] have confirmed that the initial stages of the transformation in Cu-Ti alloys was by spinodal decomposition. They have shown that the diffusion coefficient $\bar{D}$ was negative by means of microstructural observations. Since $\bar{D}$ was negative they concluded that there was spinodal decomposition.

Copper-Nickel-Tin: Schwartz [7] et al. were the first to make an electron microscope study of the Cu-Ni-Sn alloy. The as quenched alloy (Cu-9Ni-6Sn) showed glide dislocations, which tend to dissociate into Shockley partials, separated by faulted regions. There were no structural features observed that could imply decomposition of the solid solution. The 350°C aged alloy showed modulated regions which appeared to exhibit some order in their arrangement along $\langle 100 \rangle$ directions. These regions were homogeneously distributed throughout the matrix and did not tend to nucleate preferentially either at the grain boundaries or existing dislocations. The electron diffraction patterns showed sidebands along $\langle 100 \rangle$. The wavelength of the modulations increased with the aging time and the sidebands in the diffraction pattern moved closer to the main spot. On aging for 80 hours the microstructure showed regions of discontinuous precipitation interspersed with modulated regions. The discontinuous precipitates appeared to grow in a parasitic manner by consuming the modulated structure.

It was observed, in most cases that the discontinuous precipitates originated at the grain boundaries and propagated towards the grain interior. After aging for 160 hours the modulated structure was absent and the only prominent feature was the discontinuous precipitates.

Baburaj [16] et al who made a recent study of the Cu-9Ni-6Sn alloy have also reported a modulated structure in the annealed and aged material. The electron diffraction patterns showed side bands. In addition they found superlattice spots in the electron diffraction patterns indicating the formation of an ordered phase.

Plewes [2] has made an electron microscope study of the cold worked and aged alloy. The as cold worked alloy revealed a heavily tangled dislocation network with a tendency towards a loose cellular structure. After aging for 30 minutes at 350°C limited dislocation rearrangement had occurred and a more well defined cellular structure had developed. A well defined second phase network could also be resolved at high magnifications. This appeared morphologically similar to the modulated structure obtained in the annealed and aged alloy. The structure was of a completely continuous character and was uniform both in size and distribution. Electron diffraction pattern revealed broad, diffuse textured diffraction rings and side bands could not be resolved. The wavelength of the modulated structure showed little

tendency to coarsening as aging progressed. After 17 hours of aging around 70 per cent of the matrix had recrystallised. The modulated structure could be noticed even at this stage in the non recrystallised regions. Regions of lamellar discontinuous precipitates could be observed in the interiors of the recrystallised structure after prolonged aging.

2.2 Strengthening Methods for Cu-Base Alloys:

2.2.1 Strengthening by Cold Working:

Cold working is the most commonly used method of strengthening in copper base alloys since most of these alloys are not susceptible to heat treatment. The strengthening obtained by cold working is due to the process of strain hardening. Strain hardening occurs due to the interaction of dislocations with other dislocations and with other barriers to motion through the lattice. In a polycrystalline specimen because of the mutual interference of adjacent grains multiple slip occurs readily and there is appreciable strain hardening. The tensile strength and yield strength of the alloy increase and the ductility decreases with increasing amount of cold work.

The strengthening by cold working of copper has been studied by a number of workers. Wingrove [17] has studied the strengthening in pure copper. He found that on

deformation a dislocation cell structure was formed and the cell size was relatively constant above a certain value of strain. However, despite the fact that the cell size was constant, the strength continued to increase as a function of the strain. Truckner et al. [18] postulated that the strengthening in pure copper depends both on the cell size and the level of non-uniform strains associated with the dislocation substructure. They have shown by x-ray diffraction that the mean free path (i.e. cell size) associated with the dislocation substructure produced in high purity copper by rolling initially decreases and then becomes essentially constant for deformations of more than 50 per cent R.A. Beyond the point where the mean free path became constant, the material continued to work harden which could be related to the build up of the non-uniform strains in the substructure as shown by the rms microstrain determined by x-ray diffraction. The strengthening associated with dislocation substructures was expressed by an empirical relation of the form:

$$\Delta\sigma = K_1 D^{-1/2} + K_2 \left[\langle \varepsilon_L^2 \rangle^{1/2} \right]^{3/2}$$

where D - mean free path (i.e. Particle size)

$\langle \varepsilon_L^2 \rangle^{1/2}$ non uniform strain (i.e. rms microstrain)

K_1, K_2 constants

2.2.2 Strengthening by Conventional Heat Treatment:

Most of the copper base alloys are not amenable to heat treatment. However, there are some important alloys like Cu-Be which can be age hardened. The age hardening treatment consists of 1. solution treating, 2. aging. The room temperature microstructure of the alloy in the annealed condition is a two phase structure of α and β. Solution treating consists of heating the alloy above the solvus temperature in order to dissolve the β phase in the α and thus form a homogeneous solid solution. This is then quenched to room temperature in order to give a supersaturated solid solution. The aging treatment consists of heating the alloy below the solvus temperature for various lengths of time. On aging precipitation of the β phase occurs. This precipitation of second phase leads to strengthening of the alloy. The tensile strength, yield strength and hardness are increased appreciably. On further aging precipitate coarsening occurs. The coarsening leads to decrease in strength and this is called overaging.

2.2.3 Strengthening by Thermo Mechanical Treatment:

Thermo mechanical treatment (TMT) utilises plastic deformation alongwith heat treatment to modify the structural transformation and thus achieve a better combination of strength and ductility. It consists of the application of

plastic deformation either before, during or after a phase transformation. The phase transformation generally involved in copper base alloys is precipitation hardening although eutectoid hardening occurs in some Aluminium bronzes. R.R. Hart [1] and co-workers have carried out T.M.T. on Cu-base alloys. The treatment consisted of a high degree of cold work exceeding 95 per cent thickness reduction followed by a heat treatment below the recrystallisation temperature. The severe cold work resulted in increased strength due to strain hardening and texture strengthening. The heat treatment recovered the ductility while maintaining or increasing the strength imparted by cold work. The alloys studied by them include Cu-5 Sn, Cu-9Ni-2Sn, Cu-12Ni-28 Zn and Cu-2Be. In the case of Cu-5Sn they found an increase in the 0.01 per cent yield strength from 5 to 20 Ksi over the cold rolled condition due to the low temperature anneal. The extent of the increase depended upon the degree of cold rolling above 85 per cent reduction. Below 85 per cent reduction the response was less consistent and the increase in strength varied from 0 to 10 Ksi.

Tisone [19] et al. have postulated that severely cold worked material accelerates second phase precipitation during subsequent heat treatment. The increase in the yield strength was claimed to be due to this precipitation.

Caron [20] et al. have made a electron microscopic study of the strengthening by T.M.T. in Cu-5Sn bronze. They found no evidence for precipitation over the range of thermal treatments for which enhancement of the 0.01 per cent offset yield strength was exhibited. They concluded that the strength enhancement could be explained by a reduction of the mobile dislocation density by rearrangement into stable arrays and/or dislocation pinning by tin atoms.

Plewes [2] has obtained an yield strength of 175 Ksi together with a ductility of 55 per cent reduction in area in a Cu-9Ni-6Sn alloy by T.M.T. These maximum values were attained in the alloy cold rolled (99 per cent reduction in area) and aged at 350°C for 2 minutes. At higher aging time there was a reduction in both the yield strength and the ductility values. He has observed that a minimum of 75 per cent R.A. of cold work was necessary to obtain a high yield strength alongwith good ductility. Below this level of cold work the alloy was found to be brittle after T.M.T.

2.3 Mechanisms of Strengthening:

2.3.1 Spinodal Decomposition:

2.3.1.1 Basic Theoretical Concepts: Spinodal decomposition is a phase transformation in which a solid phase A separates into two other solid phases B and C. The new phases B and C have either the same crystal structure or slightly different crystal structure as the parent phase A but are of different

composition. A characteristic feature of spinodal decomposition is that the transformation occurs by uphill diffusion, that is, diffusion occurs against the concentration gradient. The phase diagram of a binary system containing a spinodal is shown in Fig. 2.4.

The mechanism of spinodal decomposition has been explained by Cahn [21] by considering the clustering phenomena. Clustering is the tendency for atoms of the same species to group together. When thermodynamic conditions are favourable for spinodal decomposition the preference for like atoms is so large that in a concentration gradient the movement of atoms is up the concentration gradient. This leads to spontaneous separation into two phase as shown in Figure 2.5. The atoms in the gradient move towards the cluster of their species and cause its concentration to increase, leaving a depleted zone around it. The outer edge of the depleted zone contains atoms that also sense a concentration gradient but away from the original particle. Because of their short range interactions they sense only the depleted zone and move away from it, building up a new cluster at a short distance away from the original one. In this way there is rapid formation of extremely small clusters approximately periodically arrayed in space.

2.3.1.2 Thermodynamics of Spinodal Decomposition: The thermodynamics of spinodal decomposition can be explained in terms

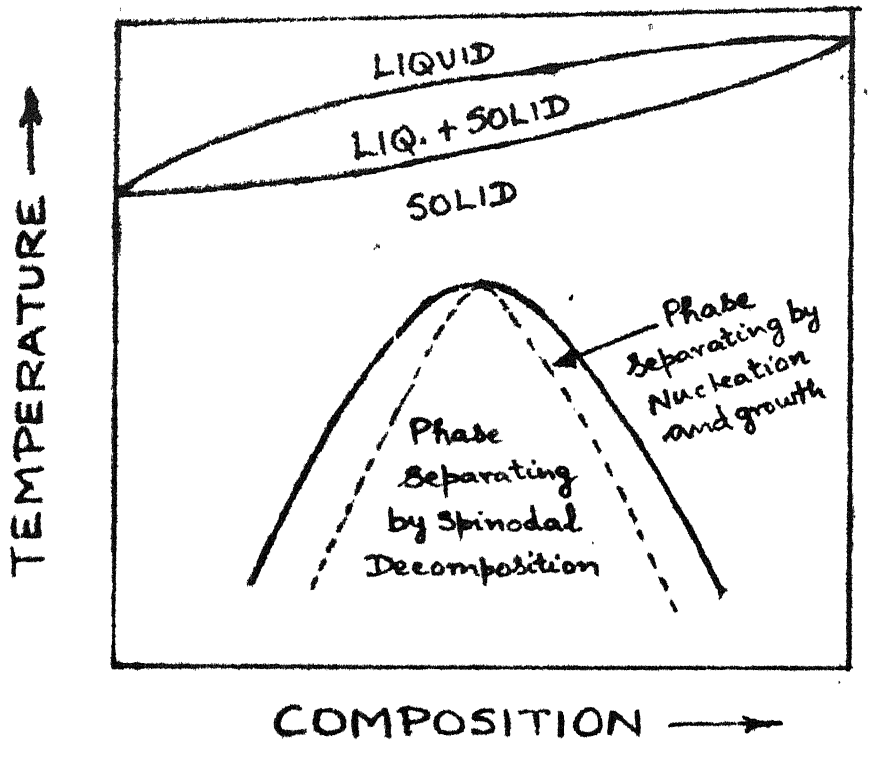

Fig. 2.4 - Binary phase diagram containing a spinodal.

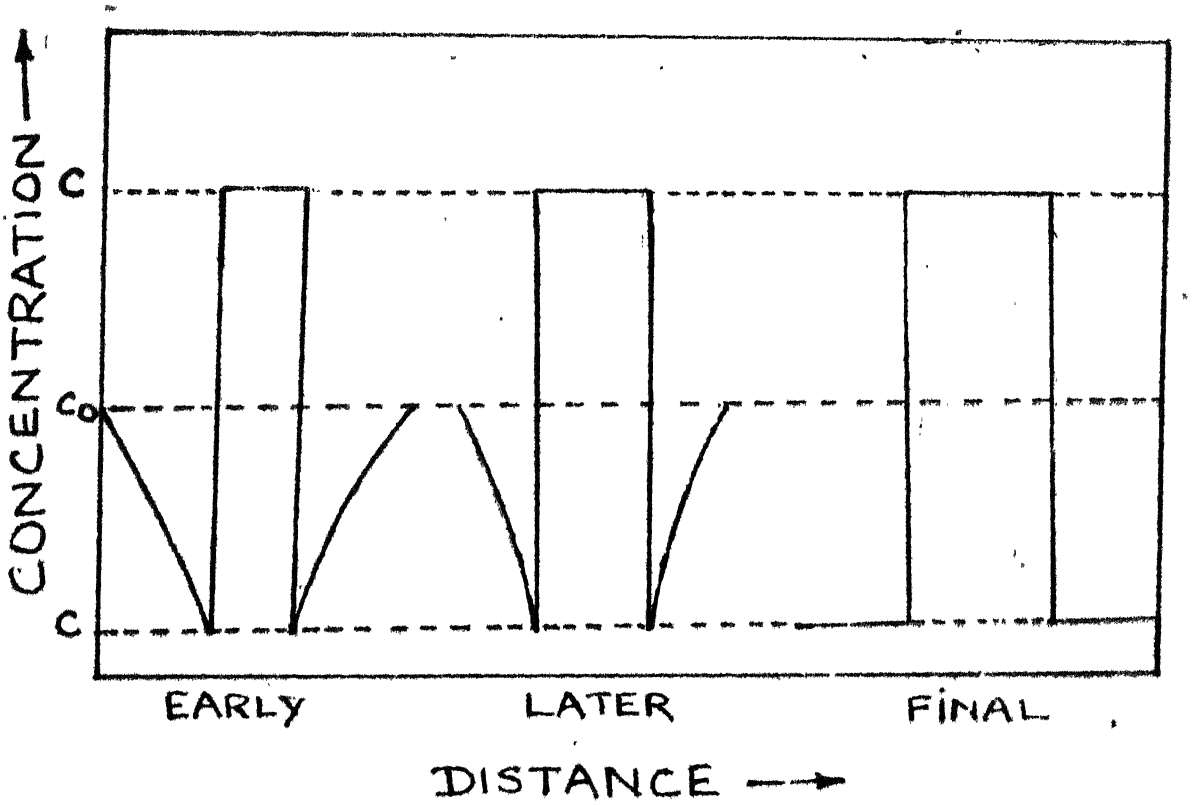

Fig. 2.5 - Mechanism of spinodal decomposition.

of free energy-composition diagrams. The free energy - composition diagrams at a temperature T_1 outside the spinodal is shown on Fig. 2.6. If there is any fluctuation in composition, the free energy of the mixture so formed is higher than the free energy of the original alloy. This indicates that the alloy outside the spinodal is metastable. The free energy-composition diagram at a temperature T_2 inside the spinodal is shown in Figure 2.7. A homogeneous phase of composition C_o is seen to be unstable, as small separations in composition about C_o all lower the free energy. Thus such separations occur spontaneously and once they have occurred are stable. The separations continue until the lowest free energy for C_o is achieved which is a two phase mixture given by the common tangent. This spontaneous trend away from homogenisation leads to a diffusional flux against the concentration gradient. The essential feature in Helmholtz free energy F which produces these effects is that the molar free energy at C_o has negative curvature. The range of negative curvature is bounded by the inflexion points in the free energy curve. The locus of the inflexion points is called the spinodal and the phase change which occurs in this is called spinodal decomposition. The inflexion points are those where the second derivative of the free energy $(\frac{\partial^2 G}{\partial C^2})T,P$ is equal to zero. The spinodal marks the limit of metastability in the system. The phase existing outside

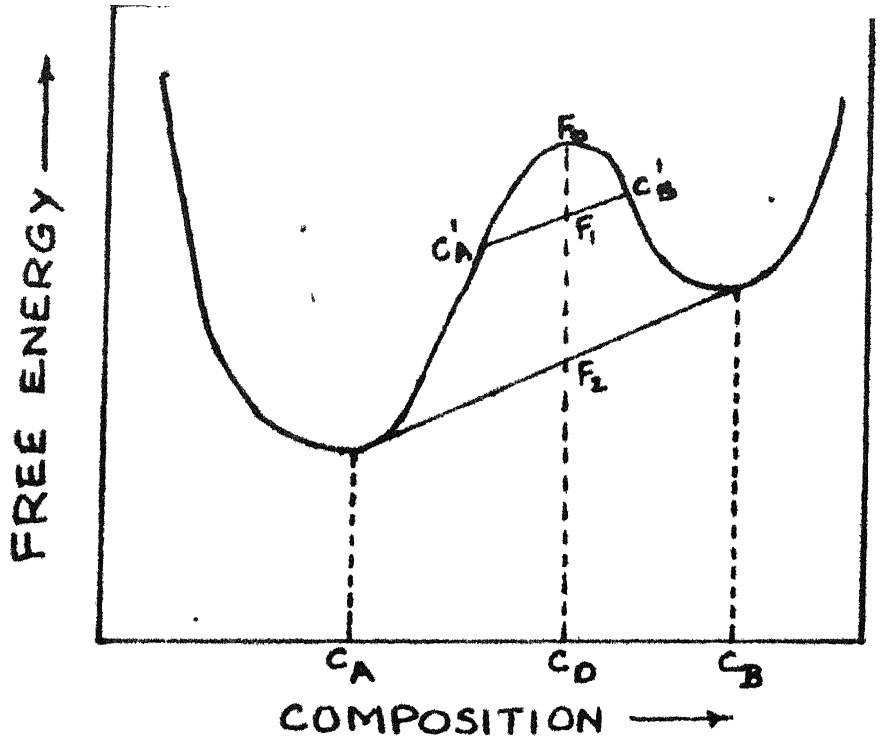

Fig. 2.6 - Free energy-composition diagram at temperatureT_1

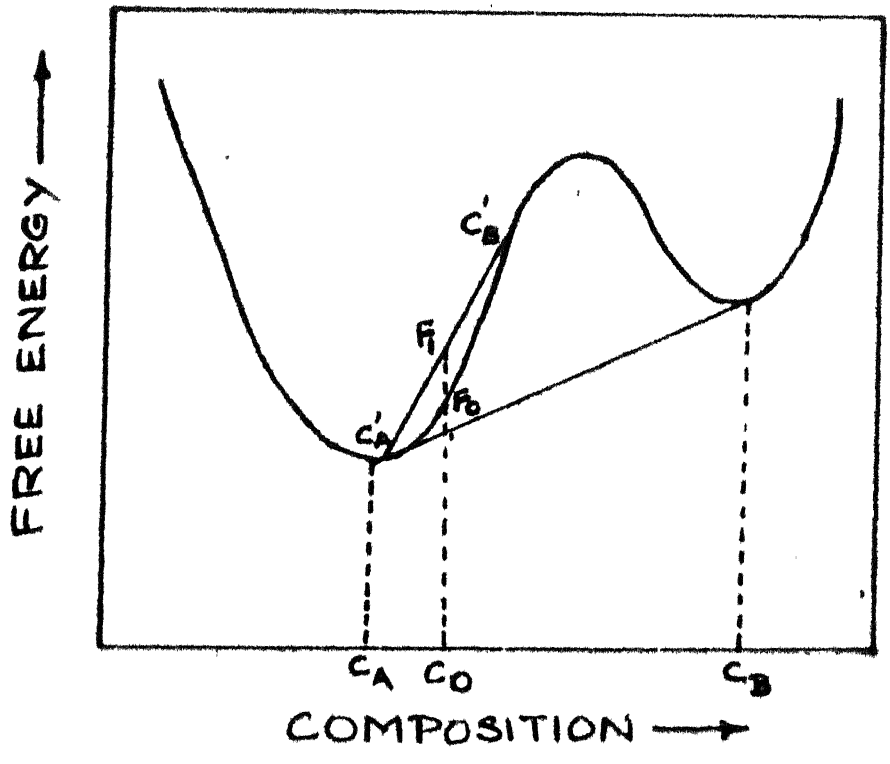

Fig. 2.7 - Free energy-composition diagram at temperature T_2

the spinodal is metastable and the phase existing inside the spinodal is unstable.

Cahn [22, 23] was the first to evolve a theory to explain spinodal decomposition. He has considered the transformation in the case of both the isotropic solid solution and in a crystal of cubic symmetry. In the case of a isotropic solid solution he [22] has shown that the difference in free energy per unit volume between the initially homogeneous solution and one with a composition fluctuation was given by

$$\frac{\Delta F}{V} = \frac{1}{4} A^2 \left[\left(\frac{\partial^2 f^1}{\partial C^2} \right) + \frac{2\eta^2 E}{1-\nu} + 2\kappa \beta^2 \right]$$

where, η = linear expansion/unit composition change,

$C - C_o = A \cos \beta_x$ is the composition fluctuation

E = Youngs modulus for the average composition

ν = Poissons ratio

$\frac{\partial^2 f^1}{\partial C^2}$ = second derivative of the Helmholtz free energy

If this was negative then the solution was unstable with respect to sinusoidal fluctuations of wavelength $2\pi/\beta$. The limit of metastability was given by the locus of

$$\frac{\partial^2 f^1}{\partial C^2} + \frac{2\eta^2 E}{1-\nu} = 0$$

This reduces to the spinodal when $\eta = 0$.

In the case of a crystal of cubic symmetry Cahn [23] showed that the free energy change per unit volume was given by

$$\frac{\Delta F}{V} = \frac{A^2}{4}\left[\frac{\partial^2 f^1}{\partial C^2} + 2\eta^2\, Y(100) + 2K\beta^2\right]$$

where $Y(100) = \dfrac{(C_{11}+2C_{12})\,(C_{11}-C_{12})}{C_{11}}$

Here Cahn [23] assumed that all anisotropies in the early stages of the decomposition were exclusively due to elastic aelotropy since there is no anisotropy in the incipient surface free energy. The above relation was valid for the elastic anisotropy factor $2C_{44}-C_{11}+C_{12} > 0$. For this condition the elastic energy was minimum for β parallel to $\langle 100 \rangle$ and the solution was expected to first become unstable to $\{100\}$ plane waves. The limit of metastability in this case was given by

$$\frac{\partial^2 f^1}{\partial C^2} + 2\eta^2\, Y(100) = 0$$

Similarly when $2C_{44}-C_{11} + C_{12} < 0$ the elastic energy was minimum when β was parallel to (111). The limit of metastability for this case was given by

$$\frac{\partial^2 f^1}{\partial C^2} + 2\eta^2\, Y(111) = 0$$

where $Y(111) = \dfrac{6(C_{11} + 2C_{12})\, C_{44}}{4C_{44} + C_{11} + 2C_{12}}$

2.3.1.3 Diffraction Effects in Spinodal Alloys: X-ray or Electron diffraction of spinodal alloys reveals 'side bands' or 'satellite' reflections. Sidebands in diffraction patterns were discovered by Bradley [24] in aged Cu-Ni-Fe alloys. These were interpreted by Daniel and Lipson [12] in terms of a 'wave-like' clustering or periodic redistribution of the solute during aging. This leads to periodic variations in the lattice spacing and scattering factor which causes the 'side bands' or 'satellite' reflections in the diffraction patterns. The wavelength λ of this modulation is given by the Daniel Lipson relationship [12].

$$\lambda = \frac{ha \tan \theta}{(h^2+k^2+l^2)\,\Delta\theta}$$

where (h,k,l) = Miller indices of the fundamental reflections.

a = Lattice parameter of the matrix,

θ = Bragg angle of the reflection

$\Delta\theta$ = Angular displacement of the sideband peak or reflection from the fundamental reflection

The sidebands have been observed in a number of spinodal alloys. Butler and Thomas [25] who have recently studied the diffraction effects in Cu-Ni-Fe alloys have confirmed the presence of sidebands along the $\langle 100 \rangle$ directions.

Cornie [11] et al. observed sidebands in Cu-Ti spinodal alloys. Laughlin [15] et al. and Dutkiewickz [13] have

confirmed the presence of sidebands along the $\langle 100 \rangle$ directions in the diffraction patterns of Cu-Ti alloys.

Schwartz [7] et al. have found 'sideband' reflections around the (111), (200) and (220) reflections in quenched and aged Cu-9Ni-6Sn alloys. The wavelength of the satellite reflections increased with the aging time and the sidebands moved closer to the fundamental reflections. Lefevre [26] et al have reported sidebands around the (200) reflection in quenched and aged Cu-15Ni-8Sn alloys.

2.3.1.4 Strengthening Effect of Periodic or Modulated Structures: Cahn [27] was the first to evolve a theory to explain the strengthening effect of modulated structures. He considered the forces on a dislocation induced by the modulated structure and concluded that the interaction of the dislocation with the elastic strain field would produce the dominant strength controlling force. In his analysis he described the structure as consisting of three mutually perpendicular $\{100\}$ cosine waves of the type $C(x)-C_o = A \cos \beta_x$. The internal stress field produced by such a sinusoidal composition wave in the x direction was given by,

$$\sigma_{yy} = \sigma_{zz} = A \eta Y (100) \cos \beta_x$$

where A = Amplitude of the modulation

β = wave vector = $\frac{2\pi}{\lambda}$, λ = wave length of modulation

$$\eta = \text{Distortion parameter} = \frac{\partial \ln a}{\partial C}$$

$$Y_{100} = Y = \frac{(C_{11} + 2C_{12})\,(C_{11}-C_{12})}{C_{11}} = \text{Youngs Modulus}$$

Cahn [27] found the force on edge and screw dislocations arising from this interaction to be far greater than that due to the effect of the gradient in the elastic modulus on the dislocation self energy or to the interfacial energy created by a cutting dislocation and neglected the latter forces. Considering the (111) [110] slip system, Cahn solved the string model of the mobile dislocation for two extreme values of the parameter $A \eta Y b / \gamma b$. For the condition $A \eta Y b/\gamma b \ll 1$ there was little bending or bowing of the dislocation and the critical resolved shear stress required to move the essentially straight dislocations through the periodically varying stress field was given by

$$\tau_o' = \frac{A^2 \eta^2 Y^2 b}{3\sqrt{6}\,\beta\,\gamma} \quad \text{(For screw dislocations)}$$

$$\tau_o'' = \frac{A^2 \eta^2 Y^2 b}{\sqrt{2}\,\beta\,\gamma} \quad \text{(For edge dislocations)}$$

The barrier to edge dislocation was about 5 times that encountered by screw components. It has been observed by a number of workers that Cahn's theory for strengthening does not tally with experimental results and was an underestimate. Due to this apparent inconsistency a number of other theories

were proposed to explain the strengthening. Ghista [28] et al. evaluated the effects of varying elastic modulus on the dislocation self energy. Their analytical procedure may be questioned as they reduce the problem to one of cylindrical symmetry by considering the interaction of a dislocation with the spatially averaged composition fluctuation Their results may be summarised as showing a dependence on A and λ of the form,

$$\sigma_{GN} \alpha \; A_{\lambda}^{-1} .$$

In attempting to fit experimental measurements of yield stress to theory, other experimenters have invoked theories which in no way should be expected to apply to spinodal alloys, as they were developed to describe the interaction of dislocations with small volume fractions of randomly dispersed spherical precipitates of a square wave compositional profile. Butler [25] et al. invoked the theory of Mott and Nabarro [29] which predicts for fixed volume fraction, $\sigma_{MN} \alpha A \eta$.

Mihalson [30] et al. used a modification of Mott and Nabarro theory which predicts for a fixed volume fraction, $\sigma_{MH} \alpha A^{3/2} \lambda^{1/2} \eta^{3/2}$.

Recent studies by Schwartz [7] et al. and Dutta [14] et. al. have shown that only Cahn's [27] theory was based on a realistic model of the early stages of the decomposition.

Sewartz [7] et al. have seriously attempted to critically analyse the mechanical strength of alloys strengthened by modulated structures. They have shown that Cahn's [27] theory essentially describes the strengthening in Cu-Ni-Sn, Cu-Ti, Au-Pt and Cu-Ni-Fe alloys to within a factor of about 2. They concluded that the strengthening predicted by Cahn's [27] model was an underestimate since the internal stress field derives from a summation over a spectrum of wave lengths. They suggest that a modification of Cahn's analysis to include the effects of a generalised composition modulation should give better agreement with experimental results.

Dutta [14] et al. who have studied the hardening in Cu-Ti alloys have also observed that Cahn's theory tends to generally underestimate the strengthening by a factor of 2. They explained that this was not surprising considering the simplifying assumptions made in the theory. They found that Cahn's theory was strictly applicable only to the early stages of the aging when a sinusoidal profile could be approximated. They conclude that in spite of these reservations, Cahn's [27] internal strain hardening model appeared to be a good first order approximation describing the mechanical strengthening due to the formation of modulated structures, regardless of the origin of these fine scale precipitates if the strengthening was derived primarily from the coherency

strain fields of the coherent composition fluctuations or particles.

2.3.2 Precipitation Hardening:

This is an important strengthening mechanism in non ferrous alloys. The phase diagram of a precipitation hardening alloy system is shown in Figure 2.1. The basic requirement of a precipitation hardening alloy system is that the solid solubility limit should decrease with decreasing temperature. The strengthening in this process is due to the precipitation of a second phase β in a supersaturated α solid solution on aging below the solvus temperature.

The electron microscope study of the phase chages occurring in Cu-Be alloy (a typical precipitation hardening alloy) has already been reported in section 2.1.3. The aging sequence observed in these alloys was G.P. zone $\longrightarrow$ intermediate precipitate $\longrightarrow$ equilibrium precipitate. The hardening in the Cu-Be alloys was associated with the formation of G.P. zones and intermediate precipitates. The softening occurred with the appearance of the equilibrium precipitate.

The hardening was due to the interaction of dislocations with the G.P. zones and precipitates. The obstacles to the motion of dislocations were 1. The strain field around

the G.P. zones, 2. The G.P. zone or precipitate themselves or both. In case the zones or precipitates themselves were involved the moving dislocation must either cut through them or go around them. Thus three major types of precipitation hardening could be identified, namely, 1. chemical hardening, 2. internal strain hardening, and 3. dispersion hardening.

The internal strain hardening mechanism was first proposed by Mott and Nabarro [29]. They pointed out that if the atomic volume of the precipitate and matrix were not the same and the precipitate was coherent with the matrix, then internal stresses may arise which would oppose dislocation motion. They evaluated the mean internal shear stress τ for the case of spherical particles containing atoms of mean atomic radius r_1 in a matrix containing atoms of mean atomic radius r_o to obtain

$$\tau = 2\ G\ \varepsilon\ f \qquad (1)$$

where,

G = shear modulus,

ε = misfit of the particle = $\dfrac{r_1 - r_o}{r_o}$, and

f = volume fraction of precipitate.

This result was independent of the size and spacing of the precipitates. They identified the flow stress with the mean internal stress so that $\tau_i = 2\ G\ \varepsilon\ f$ when the particles were of such a spacing that the radius of curvature to which

a dislocation could be bent by the mean internal stress was smaller than or equal to the spacing of the precipitate. For this condition to apply it implied that

$$d \geq b/4\ \varepsilon\ f \qquad (2)$$

where,

d = average separation of precipitate in the glide plane. b = Burgers vector of dislocation.

Mott and Nabarro have shown that if the spacing of the precipitates was less than that given by equation (2) above the flow stress would be less than that given by equation (1). They concluded that there must be a critical spacing of the precipitates for maximum strength.

The dispersion hardening theory was proposed by Orowan [31]. He assumed that the precipitates do not deform with the matrix and that the yield stress was the stress necessary to expand a loop of dislocation between the precipitates. This yield stress τ was given by,

$$\tau = \frac{G\ b}{d}$$

where,

G = shear modulus,

d = separation of the center of the particles,

b = Burgers vector of dislocation.

When this yield stress was exceeded the dislocation could move through the precipitates by leaving a loop around the precipitates.

The chemical hardening mechanism was proposed by Kelly and Fine [32]. They considered the Al - 4 per cent Cu alloy where the copper atoms tend to form zones by the clustering mechanism. They pointed out that when the dislocations pass through a zone, the number of copper - copper nearest neighbours was altered. This breaking of copper-copper bonds increased the energy of the system. They concluded that additional stress must be applied to provide this energy during slip.

CHAPTER 3

EXPERIMENTAL PROCEDURE

3.1 Material Preparation:

The alloy was prepared by induction melting of high purity Cu, Ni and Sn in Argon atmosphere. The dimensions of the ingots were 4" x 1" x 0.2". The as cast alloy was homogenised at 825°C for 50 hours in Hydrogen atmosphere. The alloy was chemically analysed and it was found to have the following composition:

Ni : 8.82 weight per cent

Sn : 6.12 weight per cent

Cu : Balance

3.2 Cold Rolling:

The alloy was cold rolled on a 2-high laboratory rolling mill using paraffin oil as a lubricant. The strips were reversed end to end after each pass. In between any two successive passes the strips were dipped into a bowl of cold water to minimise temperature rise due to deformation as far as practicable. The material was rolled to 95 per cent reduction in thickness.

3.3 Preparation of Tensile Samples:

Tensile samples were prepared from the cold rolled material. The dimensions of the tensile sample are shown in Figure 3.1.

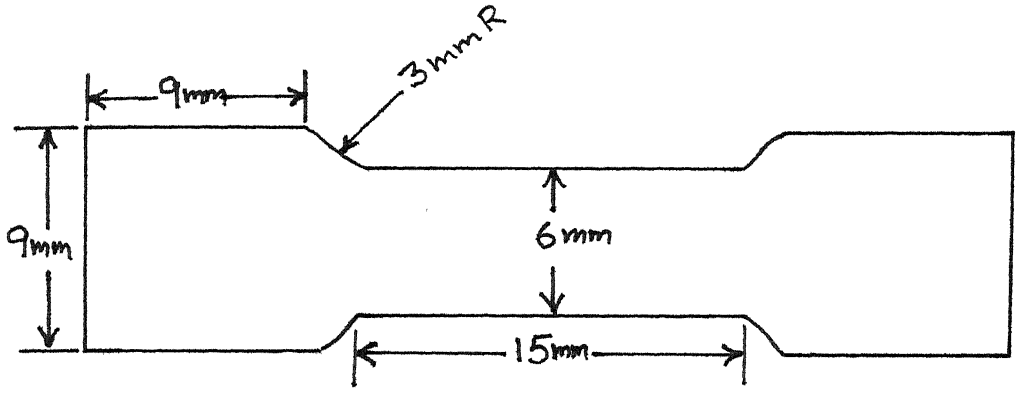

Fig. 3.1. TENSILE SAMPLE

3.4 Heat Treatment:

The heat treatment was carried out in a pot furnace using a Alumel-Chromel thermocouple connected to a Leeds and Northrup temperature controller. A salt bath consisting of an eutectic mixture of 50 per cent sodium nitrate and 50 per cent potassium nitrate in a stainless steel crucible was used to prevent oxidation of the samples. The tensile samples were aged at 350°C and 600°C for various lengths of time. Small strips cut from the rolled sheet were also aged at 350°C and 600°C for various lengths of time. These strips were used for electron microscopy, X-ray diffraction and optical microscopy.

Another batch of tensile samples were annealed in a tube furnace at 825°C for 30 minutes using an Argon atmosphere. The annealed samples were aged at 350°C for various lengths of time. Small strips cut from the rolled sheet were also annealed at 825°C and then aged at 350°C for various lengths of time. These strips were used for electron microscopy, x-ray diffraction and optical microscopy.

3.5 Optical Microscopy:

The samples were mounted on perspex blocks using cold setting resin. They were polished using different grades of emery paper and were given a final polish on the lap. The samples were etched using a etchant of the following composition:

$4:4:5::NH_3:H_2O_2:H_2O$

The etched specimens were observed under an optical microscope and the microstructure was recorded on photographic film.

3.6 Electron Microscopy:

The electron microscopy was carried out in a Philips EM 301 machine operated at 100 KV. Foils were made from the rolling plane sections. The material was given an initial chemical thinning in a 50 per cent HNO_3 : 50 per cent H_2O mixture to reduce it to about 0.005 inch thickness. This was then electropolished using an electrolyte comprising of acetic acid and nitric acid in the ratio of 2:1. The bath was maintained at sub-zero temperatures using ice and liquid nitrogen. The voltage used was 15-17 volts. A thin stainless steel rod bent into the form of an U was used as the cathode. The foils so made were enclosed within the grids and examined under the microscope.

3.7 X-Ray Diffraction:

The x-ray diffraction was carried out in a General electric XRD-5 diffractometer. The machine was operated at 35 KV and 18 mA using a coblat target and iron filter. The specimens were of the size (1" x 3/4") and the scanning was carried out between 30° and 100°. The diffracted intensity was measured with a proportional counter and was

displayed on a chart recorder.

3.8 Differential Thermal Analysis:

Differential thermal analysis was performed on the annealed sheet material. In this technique the sample temperature was continuously compared, during heating, with the temperature of a reference specimen and the difference in temperature recorded as a function of temperature. The sample and the reference material were heated in close proximity by placing them in separate chambers in small cups mounted on the tips of thermocouples. The experiments were carried out in a Derivatograph. The material to be analysed was in the form of small disks, about 0.15" side cut out from the annealed sheets. These were given a slight chemical polish in 50:50 HNO_3:H_2O mixture, washed in water and alcohol and dried. These were then put in one of the container cups. The other cup contained an equal weight of reference material i.e. 95 per cent cold rolled copper sheets in the fully recrystallised condition. The heating of the specimen and the reference material was done under a blanket of Argon to avoid oxidation at a rate of $5^{\circ}C$/min upto $700^{\circ}C$.

3.9 Tensile Testing:

The tensile testing was carried out on an Instron testing machine at a cross head speed of .05/min. and a strain rate of .033/min.

3.10 Scanning Electron Microscopy:

The fractured surfaces of a few cold worked and aged tensile specimens were examined using a Cambridge 'Streoscan' scanning electron microscope.

CHAPTER 4

EXPERIMENTAL RESULTS

4.1 Results of Mechanical Testing:

The results of mechanical testing are shown in tabular form in Tables 4.1 to 4.3 and graphically in Figures 4.1 to 4.3.

4.1.1 Cold Rolled and Aged at 350°C:

Yield Strength (Y.S.): The 95 per cent cold worked alloy is found to have a 0.2 per cent yield strength of 115.8 Ksi. The yield strength values increase steadily from the cold worked value for the samples aged at 350°C for shorter time intervals upto 1 minute. For the 1 minute aged sample the Y.S. is 129.9 Ksi. There is a sharp increase in the value to 150.1 Ksi for the 5 minutes aged sample. The Y.S. further increases to give a maximum value of 168 Ksi after 10 minutes aging. It decreases slightly to 160.5 Ksi after 30 minutes aging. There is a further fall to 150.1 Ksi after 1 hour aging. The Y.S. decreases steadily to 136 Ksi after 6 hours aging, 134.0 Ksi after 15 hours aging, and 132.5 Ksi after 20 hours aging.

Ultimate Tensile Strength (U.T.S.): The U.T.S. of the cold rolled alloy is 141.5 Ksi. It increases sharply to

TABLE 4.1: MECHANICAL PROPERTIES OF Cu-9Ni-6Sn ALLOY 95 PER CENT COLD ROLLED AND AGED AT 350°C

Aging Time	Yield strength in Kg/mm^2	Yield strength in KSi	Ultimate tensile strength in Kg/mm^2	Ultimate tensile strength in Ksi	Percentage elongation
As rolled	81.4	115.8	99.4	141.5	2.7
10 secs.	82.6	117.6	94.5	134.4	2.7
20 secs.	85.8	122.0	114.3	162.5	2.9
30 secs.	88.2	125.4	115.7	164.6	2.9
1 min.	91.4	129.9	115.7	164.6	2.9
5 min.	105.5	150.1	118.1	168.0	3.1
10 min.	118.1	168.0	132.3	188.1	3.3
30 min.	112.9	160.5	117.8	167.5	4.4
1 hour	105.5	150.1	115.7	164.6	4.8
2 hours	101.9	145.0	116.8	166.0	4.8
4 hours	99.5	141.5	115.2	164.0	4.3
6 hours	95.6	136.0	114.1	162.2	4.9
15 hours	94.2	134.0	113.4	161.0	5.2
20 hours	93.2	132.5	112.9	160.5	5.3

TABLE 4.2: MECHANICAL PROPERTIES OF Cu-9Ni-6Sn ALLOY 95 PER CENT COLD ROLLED AND AGED AT 600°C

Aging Time	Yield strength in Kg/mm^2	Yield strength in Ksi	Ultimate tensile strength in Kg/mm^2	Ultimate tensile strength in Ksi	Percentage elongation
3 secs.	81.9	116.4	88.2	125.4	8.3
5 secs.	66.2	94.0	72.4	103.0	5.3
10 secs.	75.6	107.5	80.6	114.2	8.8
30 secs.	56.7	80.6	74.0	105.2	14.6
1 min.	53.5	76.1	65.4	92.9	12.0
5 mins.	34.6	49.3	53.5	75.9	14.0
10 mins.	28.3	40.3	47.3	67.2	19.8

TABLE 4.3: MECHANICAL PROPERTIES OF Cu-9Ni-6Sn ALLOY ANNEALED AND AGED AT 350°C

Aging Time	Yield strength in Kg/mm^2	Yield strength in Ksi	Ultimate tensile strength in Kg/mm^2	Ultimate tensile strength in Ksi	Percentage elongation
As annealed	23.0	32.7	38.9	55.2	16.7
2 mins.	35.9	51.0	40.9	58.1	15.1
10 mins.	54.2	77.0	62.1	88.4	12.0
20 mins.	61.1	86.9	70.0	99.5	14.8
2 hours	46.6	66.4	65.8	93.6	14.2
4 hours	45.3	64.4	59.1	84.2	14.0
6 hours	42.5	60.5	57.3	81.5	13.8
15 hours	41.9	59.7	55.0	78.2	9.1
20 hours	41.7	59.3	51.2	77.5	5.6

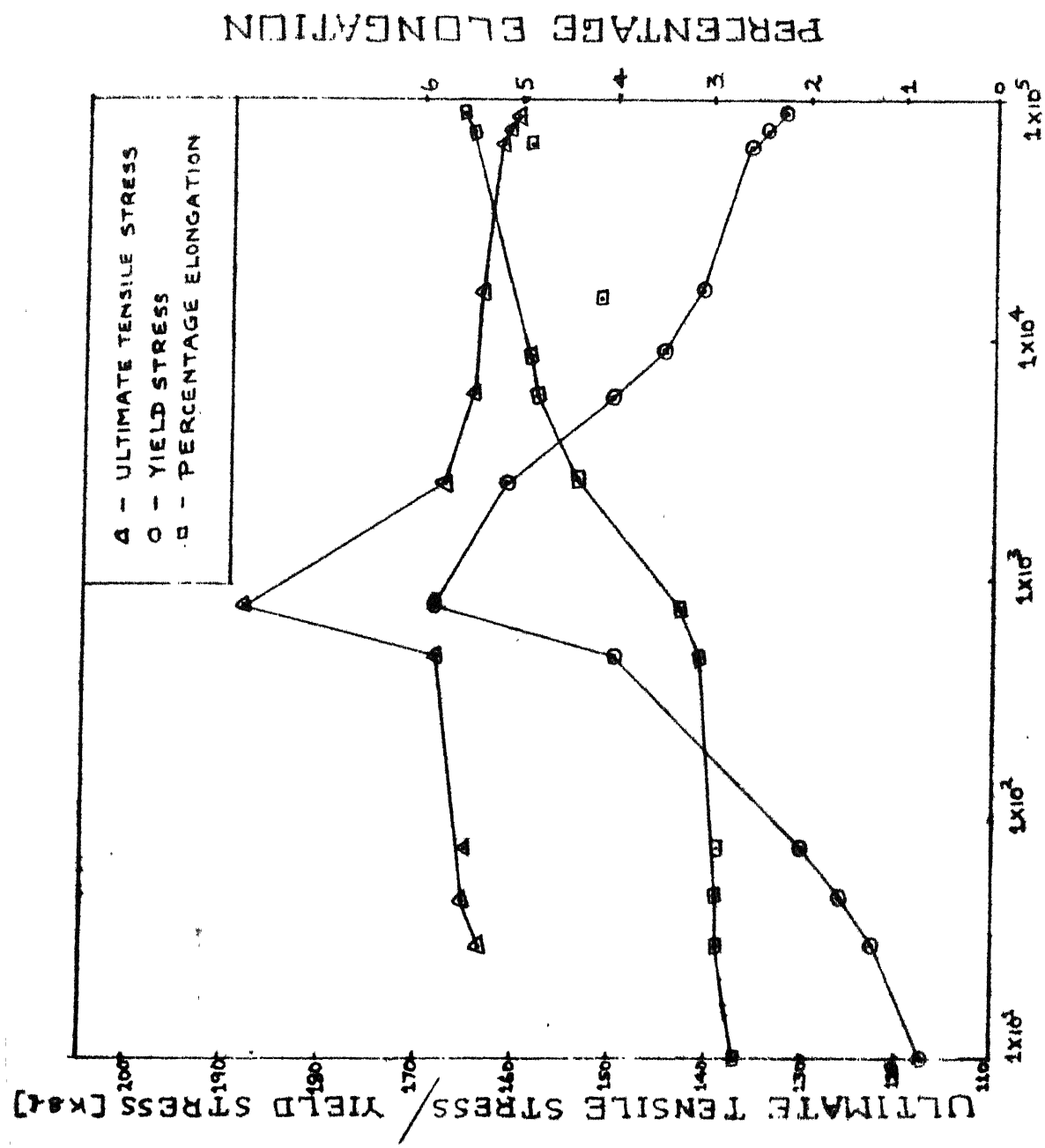

Fig. 4.1 – Mechanical properties of cold rolled and aged at 350°C, Cu – 9Ni–6Sn alloy.

162.5 Ksi after 20 seconds aging and remains practically constant at the same value upto 1 minute aging. There is a slight increase in the value to 168 Ksi after 5 minutes aging. The U.T.S. increases sharply to a maximum value of 188 Ksi after 10 minutes aging. After 30 minute aging a sharp fall in the U.T.S. to 167.5 Ksi is noticed. The U.T.S. is practically constant with values between 161-166 Ksi upto 15 hours aging. After 20 hours aging the U.T.S. value is 160.5 Ksi.

Percentage Elongation: The P.E. of the cold rolled material is 2.7. This is practically constant upto 20 minutes aging. After 30 minutes aging there is an increase in the value to 4.1. This is constant upto 6 hours aging. There is a steady increase in the P.E. with further aging. The maximum value of P.E. of 5.3 is attained after 20 hours aging.

4.1.2 Cold Rolled and Aged at 600°C:

Yield Strength (Y.S.): The Y.S. of the cold rolled material is 115.8 Ksi. It increases slightly to 116.4 Ksi after 3 seconds aging. The Y.S. decreases sharply to 107.5 Ksi after 10 seconds and 80.6 Ksi after 30 seconds aging. The decreasing trend is maintained at higher aging time. It decreases steadily to 76.2 Ksi after 1 minute and 49.3 Ksi after 5 minutes aging. After 10 minutes aging the Y.S. is 40.3 Ksi which is close to the annealed value.

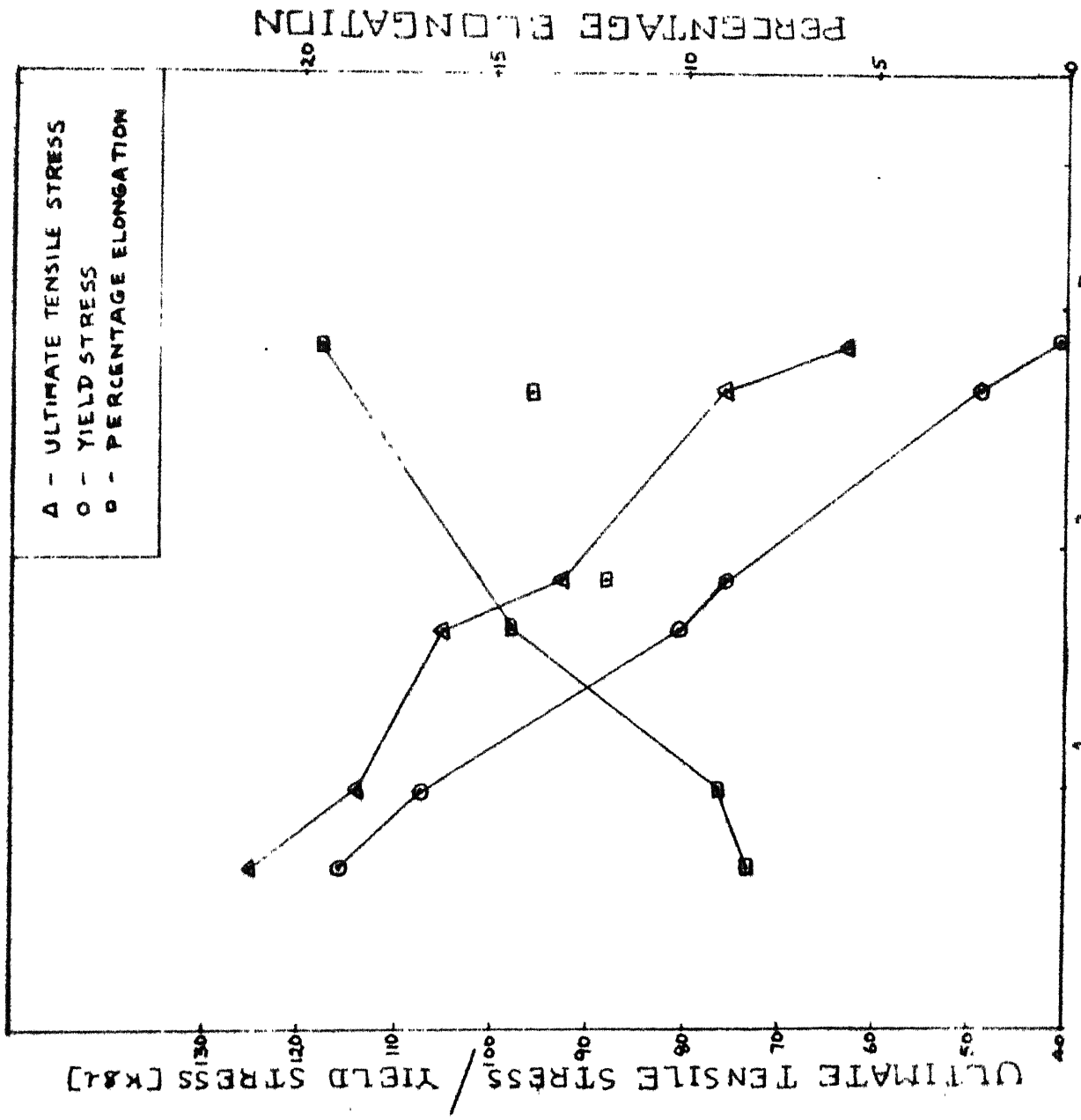

Fig. 4.7 - Mechanical properties of cold rolled and aged at 600°C, Cu-9Ni-6Sn alloy.

Ultimate Tensile Strength (U.T.S.): The U.T.S. of the cold rolled alloy was 141.5 Ksi. There is a sharp decrease in this value to 125.4 Ksi even after 3 seconds aging. On further aging the U.T.S. decreases sharply to 114.2 Ksi after 10 seconds, 105.2 Ksi after 30 seconds and 92.9 Ksi after 1 minute aging. The decreasing trend is maintained for higher aging time. It decreases steadily to 75.9 Ksi at after 5 minutes aging and 67.2 Ksi after 10 minutes aging.

Percentage Elongation (P.E.): The P.E. of the cold rolled alloy is 2.7. There is a sharp increase in the value to 8.3 even after 3 seconds aging. It increases further to 8.8 after 10 seconds and 14.6 after 30 seconds aging. There is a slight decrease to 12.0 after 1 minute aging. The P.E. value again increases to 14.0 after 5 minutes aging and a maximum value of 19.8 is attained after 10 minutes aging.

4.1.3 Annealed and Aged at 350°C:

Yield Strength (Y.S.): The Y.S. of the annealed material is found to be equal to 32.7 Ksi. It increases sharply to 51 Ksi at 2 minutes aging and 77.0 Ksi after 10 minutes aging. It increases further to give a maximum value of 86.9 Ksi after 20 minutes aging. The Y.S. decreases sharply to 66.4 Ksi after 2 hours aging. The decreasing trend is maintained at higher aging time. The Y.S. decreases steadily to 64.4 Ksi after 4 hours and 60.5 Ksi after 6 hours

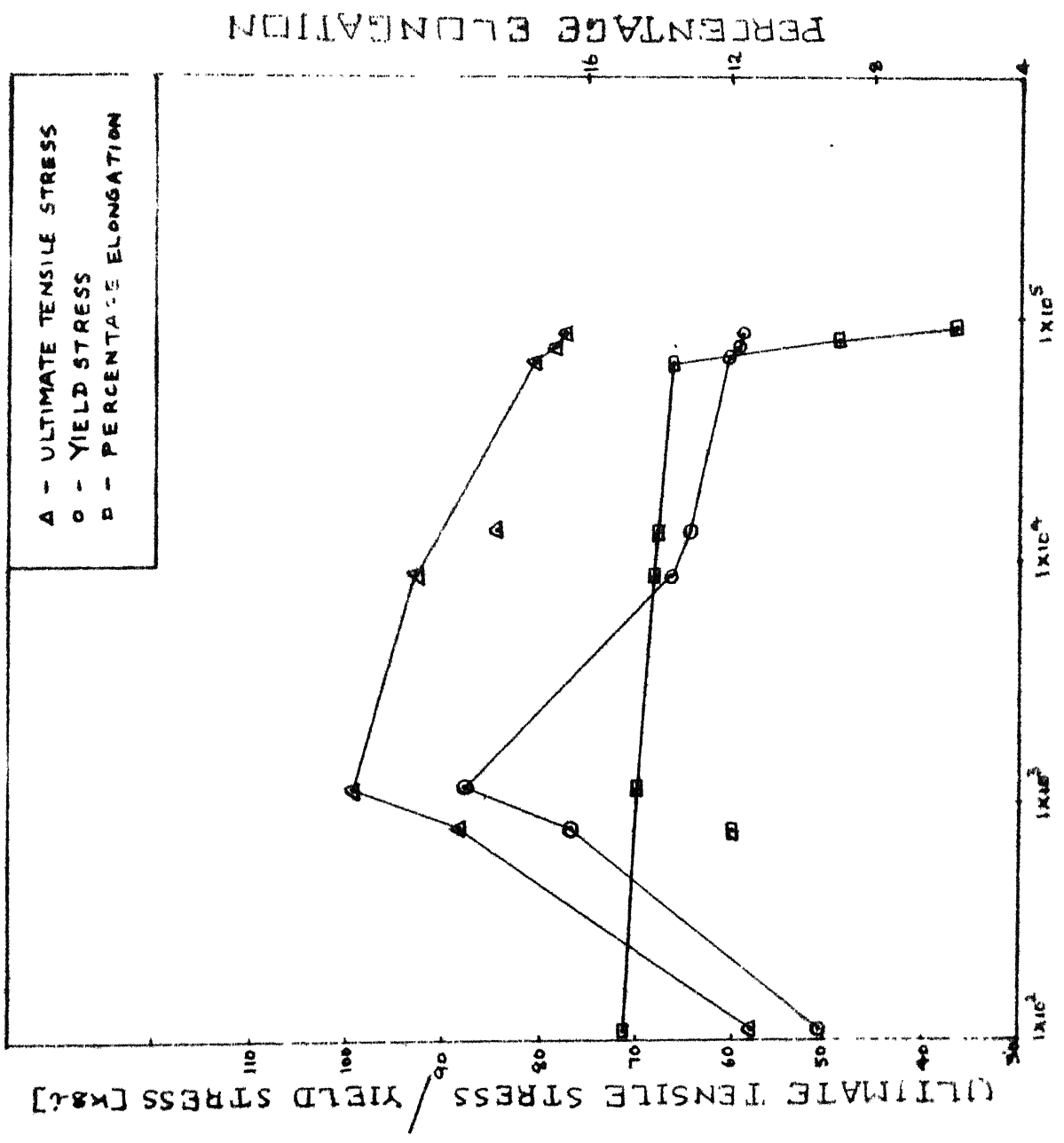

Fig. 4.3 - Mechanical properties of annealed and aged at 350°C, Cu-9Ni-6Sn alloy.

of aging. The Y.S. is practically constant upto 20 hours aging which gives a value of 59.3 Ksi.

Ultimate Tensile Strength (U.T.S.): The U.T.S. of the annealed material is 55.2 Ksi. It increases slightly to 58.1 Ksi after 2 minutes aging. There is a sharp increase to 88.4 Ksi after 10 minutes aging. The maximum value of 99.5 Ksi is attained after 20 minutes aging. The U.T.S. decreases slightly to 93.6 Ksi after 4 hours aging. The decreasing trend is maintained for higher aging time and a U.T.S. value of 77.5 Ksi is obtained after 20 hours aging.

Percentage Elongation (P.E.): The P.E. of the annealed material is 16.7. This decreases to 15.1 after 2 minutes aging and remains practically constant at this value upto 6 hours of aging. There is a sharp fall in the value to 9.1 after 15 hours aging and the lowest value of 5.6 is obtained after 20 hours aging.

4.2 Optical Microstructures:

Figure 4.4 shows the microstructure of the cold worked alloy. At this stage highly deformed and elongated grains can be seen. Presumably the grains are elongated along the rolling direction. The microstructure of the alloy cold rolled and aged at 350°C for 10 minutes is shown on Figure 4.5. There is not much change from the cold worked structure. Figure 4.6 shows a similar microstructure for the alloy aged

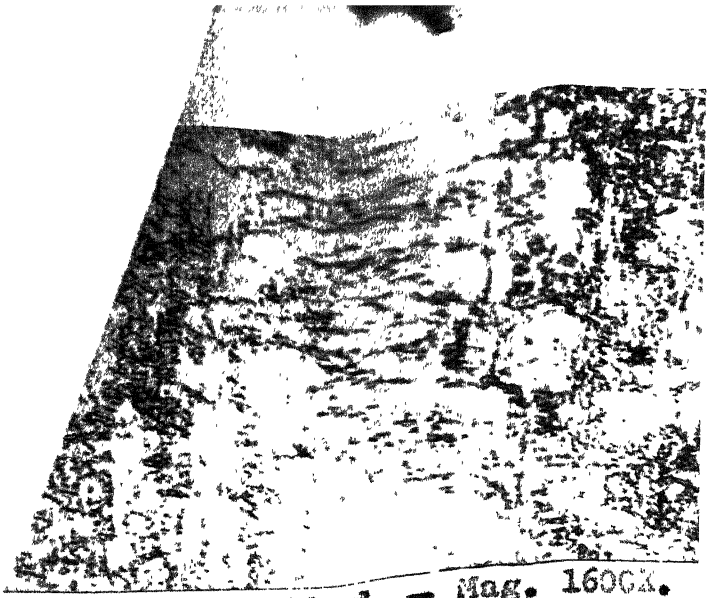

e.4.4 : Cold Rolled – Mag. 1600X.

Fig. 4.5: Cold Rolled and Aged at 350°C for 10 minutes – Mag. 1600X.

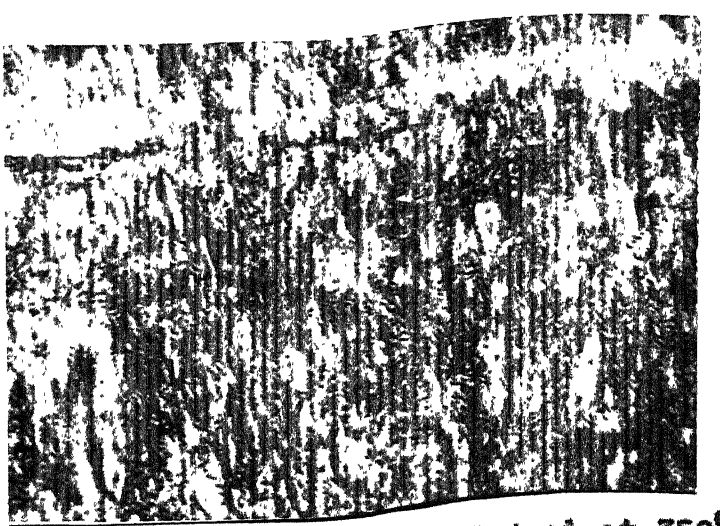

Fig. 4.6: Cold Rolled and Aged at 350°C for 1 hour – Mag. 1600X.

for 1 hour at this temperature. However, after aging for 10 hours the microstructure (Fig.4.7) shows the precipitation of a second phase in the cold worked matrix. Extensive precipitation is noticed after 30 hours of aging at 350°C (Fig.4.8).

The microstructure (Figure 4.9) of the alloy annealed at 825°C for 30 minutes shows recrystallised grains of various sizes. Twins can also be observed in some grains.

The nature and morphology of the precipitate particles at the early stages of aging are not very clear from the optical micrographs. In order to have a clearer idea about their nature extensive electron microscopy of thin foils of the material at different stages of aging was carried out.

4.3 Electron Microstructures:

Figure 4.10 shows the electron micrograph of the 95 per cent cold worked alloy. At this stage the cell structure is elongated and the elongation seems to be parallel to the rolling direction. The micrograph from another area is shown in Figure 4.11. The structure shows a profusion of micro-twins presumably due to the severe cold work. The SAD from the cold worked area is shown in Figure 4.12. Figures 4.13 to 4.23 are the micrographs of the alloy that has been cold rolled and aged at 350°C for various lengths of time. Figure 4.13 shows the micrograph of the alloy aged for 1 minute. The cell structure of the cold worked state is

Fig. 4.7: Cold Rolled and aged at 350°C for 10 hours - Mag. 1600X.

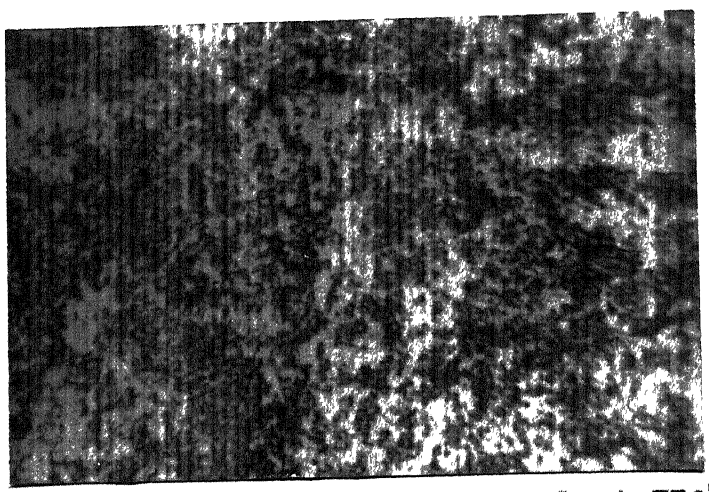

Fig. 4.8: Cold rolled and aged at 350°C for 30 hours - Mag. 1600X.

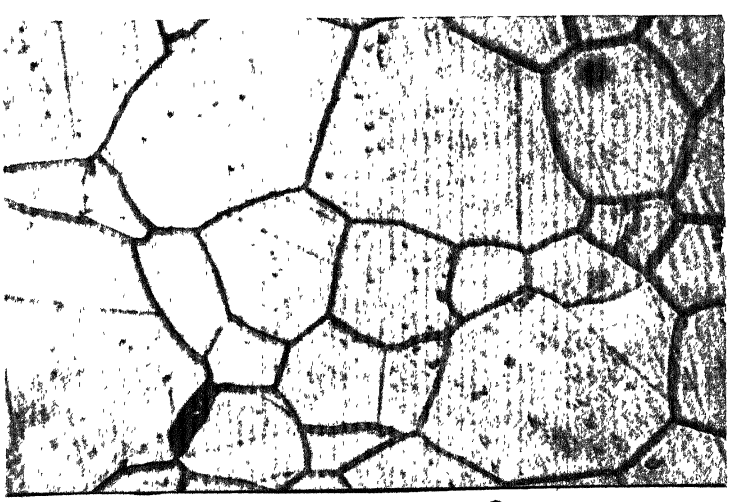

Fig. 4.9: Annealed at 825°C for 30 minutes - Mag. 1600X.

Fig. 4.10: Cold rolled - Mag. 15,300X.

Fig. 4.11: Cold rolled - Mag.51,000X.

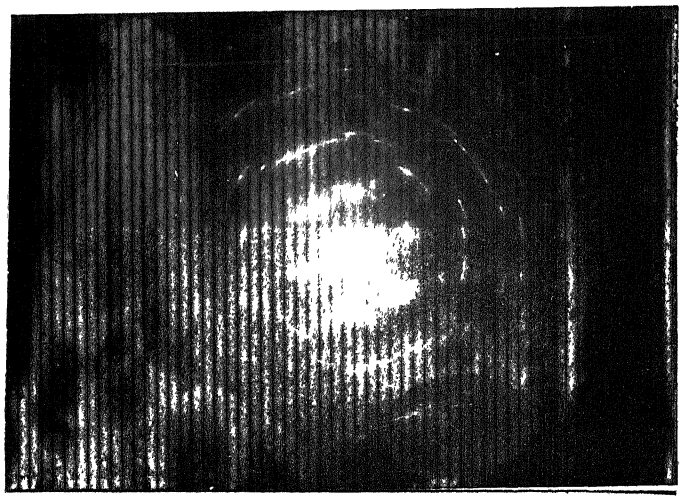

Fig. 4.12: Cold rolled

maintained. In addition a fine precipitation can be noticed in the matrix. Figure 4.14 shows the microstructure of the alloy that has been aged for 10 minutes. The dislocatio cell structure of the cold worked state is retained along with a fine matrix precipitation. Alternate dark and bright streation contrast can also be noticed at a few places. The micrograph of the alloy that has been aged for 20 minutes is shown in Figure 4.15. The cold worked structure is retained and twins can also be noticed at a few places. Figure 4.16 shows the SAD from the above area. The microstructure of the alloy that has been aged for 30 minutes is shown in Figure 4.17. The structure shows a large number of fringes. The fringe separation is of the order of 50-100 $\mathring{A}$. The corresponding SAD pattern is shown in Figure 4.18. The micrograph of the alloy that has been aged at 350°C for 1 hour is shown on Figure 4.19. The contrast obtained at this stage is similar to that shown by a spinodal decomposition product. Figure 4.20 shows the microstructure of the alloy that has been aged at 350°C for 2 hours. A fine matrix precipitation can be clearly noticed. The dislocation cell structure of the cold worked state is retained. In addition alternate dark and bright contrast streations are visible at many places. The micrograph of the alloy aged for 20 hours is shown in Figure 4.21. At this stage precipitates can be noticed in the cold worked matrix. Figure 4.22 shows the micrograph

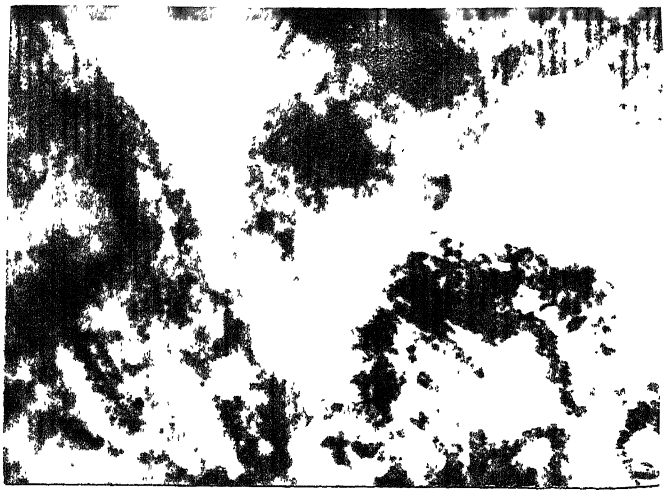

Fig. 4.13: Cold rolled and aged at 350°C for 1 minute - Mag. 51,000X.

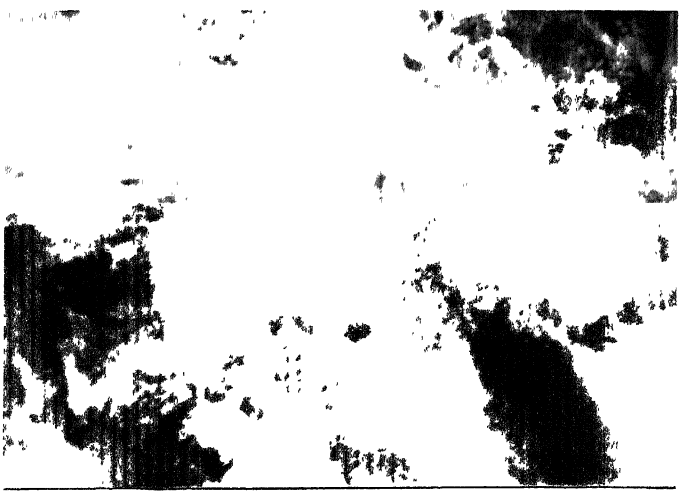

Fig. 4.14: Cold rolled and aged at 350°C for 20 minutes - Mag. 51,000X.

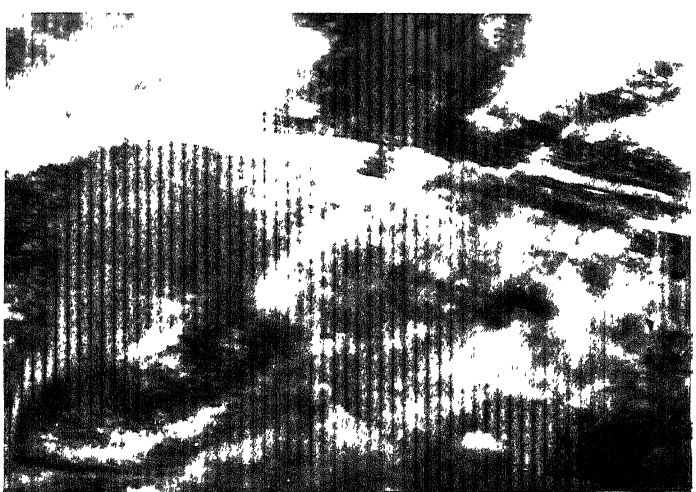

Fig. 4.15: Cold rolled and aged at 350°C for 20 minutes - Mag. 51,000X.

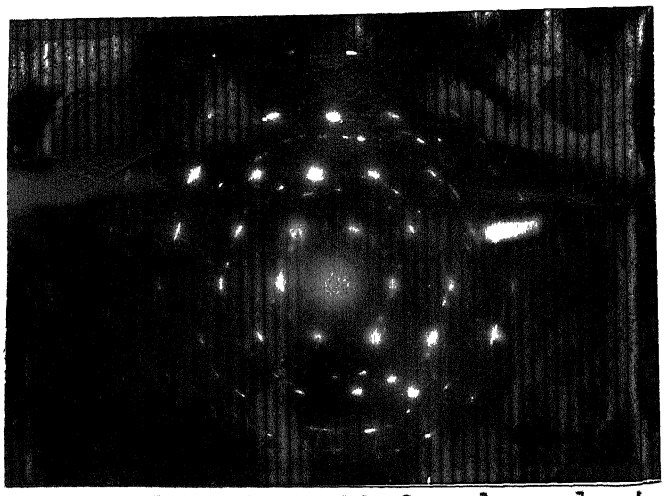

Fig. 4.16: Cold rolled and aged at 350°C for 20 minutes

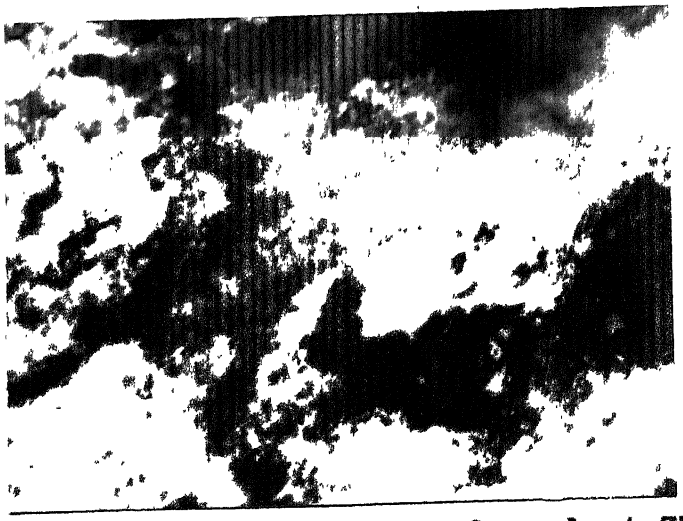

Fig. 4.17: Cold rolled and aged at 350°C for 30 minutes - Mag. 84,000X

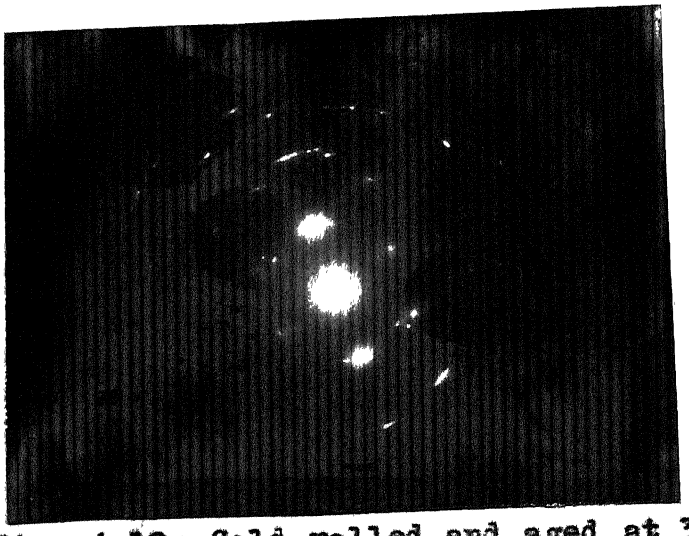

Fig. 4.18: Cold rolled and aged at 350°C for 30 minutes

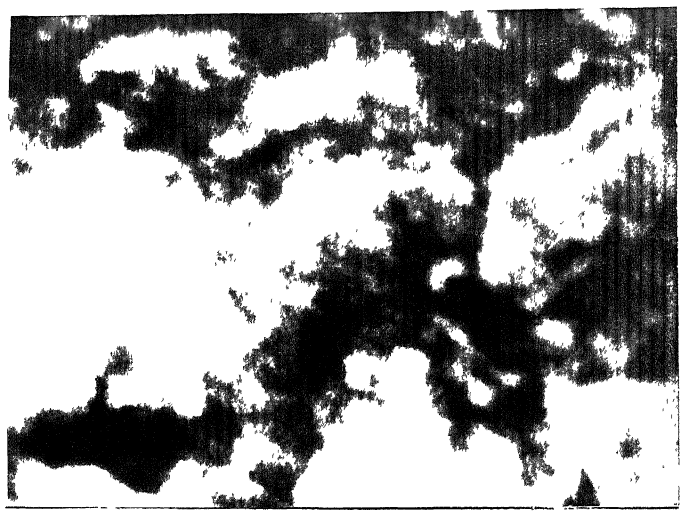

Fig. 4.19: Cold rolled and aged at 350°C for 1 Hour - Mag. 66,000X.

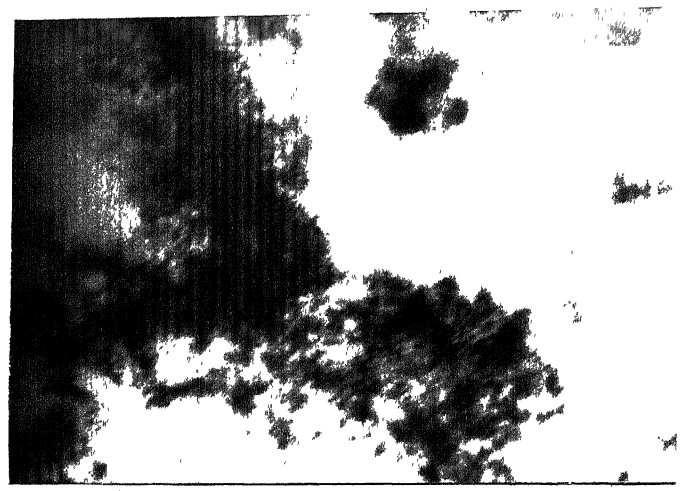

Fig. 4.20: Cold rolled and aged at 350°C for 2 Hours - Mag. 117, 000X.

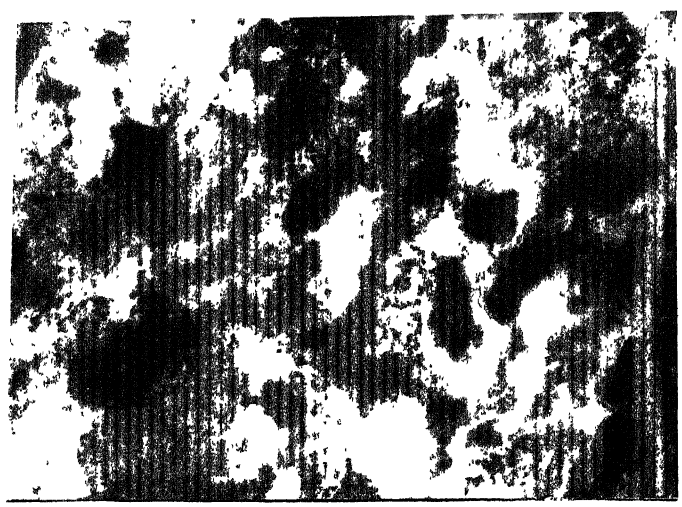

Fig. 4.21: Cold rolled and aged at 350°C for 20 hours - Mag. 51,000X.

from another area. This area shws a profusion of precipitates. The corresponding SAD is shown in Figure 4.23. On analysis it is seen that the precipitates are of an ordered phase. Discontinuous precipitates of varying sizes and morphologies can be seen on aging for 50 hours and 100 hours. (Figures 4.24 and 4.25).

Figure 4.26 shows the micrograph of the alloy that has been cold rolled and aged at 600°C for 10 seconds. At this stage a few dislocation free subgrains are present in the cold worked matrix. The matrix also shows a certain amount of recovery. The micrograph of the alloy that has been aged at 600°C for 1 minute after cold working is shown in Figure 4.27. The structure shows recrystallised grains growing into the cold worked areas. Lumpy precipitates can be seen both inside and at the boundaries of the recrystallised grains. Some precipitates can also be observed in the cold worked areas. The micrograph of another area is shown in Figure 4.28. This shows a distribution of precipitates of different morphologies within the recrystallised grains. Figure 4.29 shows the micrograph of the alloy that has been aged for 10 minutes at the above temperature after cold rolling. The structure shows recrystallised regions with very few small cold worked areas. Precipitates can be observed in the recovered regions. In some regions the precipitates are small and bigger precipitates are observed in other regions.

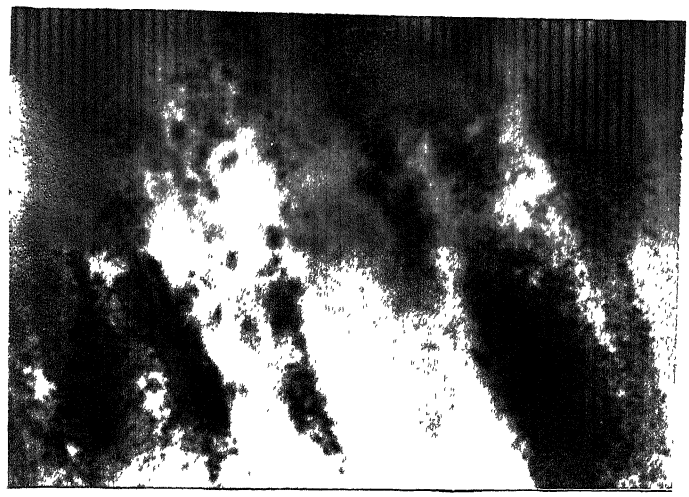

Fig. 4.22: Cold rolled and aged at 350°C for 20 Hours - Mag. 39,000X.

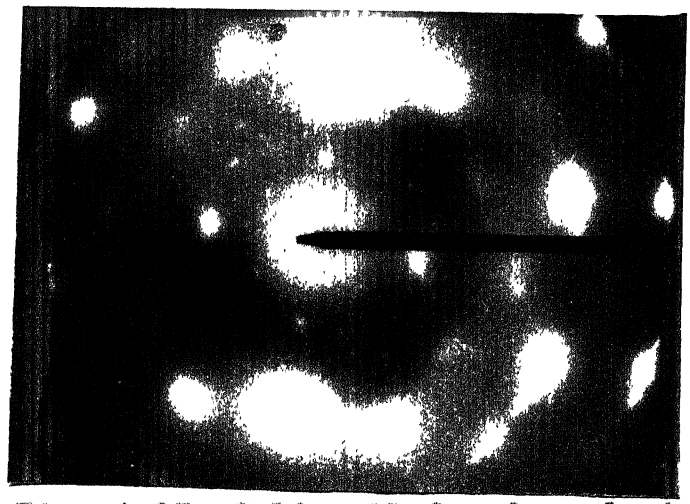

Fig. 4.23: Cold rolled and aged at 350°C for 20 hours

Fig. 4.24: Cold rolled and aged at 350°C for 50 hours - Mag. 39,000X.

Fig. 4.25: Cold rolled and aged at 350°C for 100 hours - Mag. 30,000X.

Fig. 4.26: Cold rolled and aged at 600°C for 10 seconds - Mag. 51,000X.

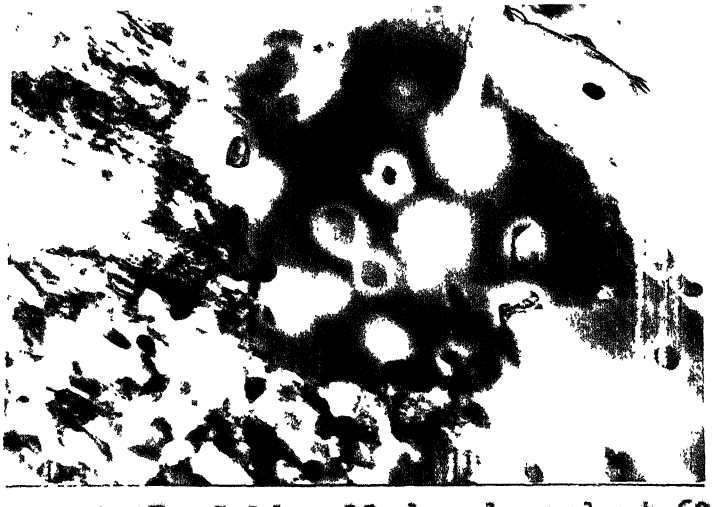

Fig. 4.27: Cold rolled and aged at 600°C for 1 minute - Mag. 21,400X.

Fig. 4.28: Cold rolled and aged at 600°C for 1 minute - Mag. 15,300X.

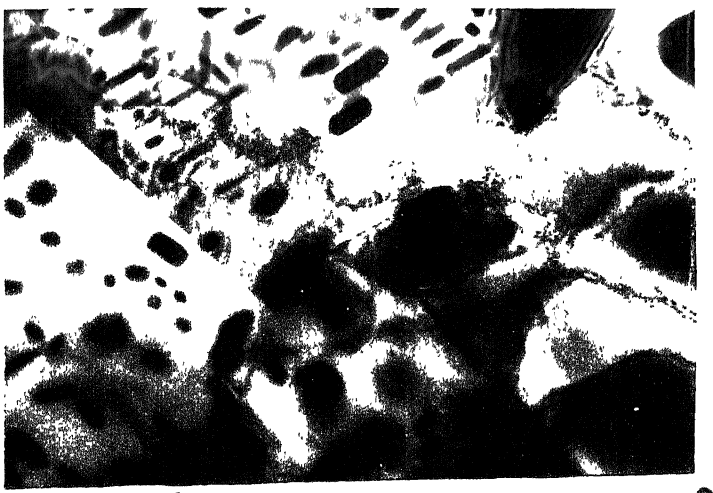

Fig. 4.29: Cold rolled and aged at 600°C for 10 minutes - Mag.21,400X.

Fig.4.30: Annealed at 825°C for 30 minutes - Mag. 84,000X.

Figure 4.30 shows the micrograph of the alloy that has been annealed at 825°C for 30 minutes. The structure shows almost defect free solid solution. Isolated dislocations can be seen at a few places in the matrix. Figures 4.31 to 4.46 are the micrographs of the alloy that has been annealed and aged at 350°C for various lengths of time. Figure 4.31 is the micrograph of the alloy that has been aged for 10 minutes. At this stage a modulated structure is obtained which is a spinodal decomposition product. The corresponding SAD, shown in Figure 4.32, indicates side band formation for the (200) spots. The micrograph of the alloy aged for 30 minutes is shown in Figure 4.33. The modulated structure typical of a spinodal decomposition product is again observed. Figures 4.34 to 4.36 are the SAD's from different areas. In addition to the formation of side bands they reveal a few superlattice reflections. Figure 4.35 shows a square pattern of superlattice spots while Figure 4.36 shows a hexagonal pattern of spots. Figure 4.37 shows the micrograph of the alloy aged for 1 hour. A modulated structure is again obtained. The corresponding SAD shown in Figure 4.38, has a few extra reflections which may be due to superlattice reflection. The micrograph of the alloy that has been aged for 2 hours is shown in Figure 4.39. It shows 3 different grains. Tabular precipitates can be noticed both inside the grains and at the grain boundaries. An interesting feature

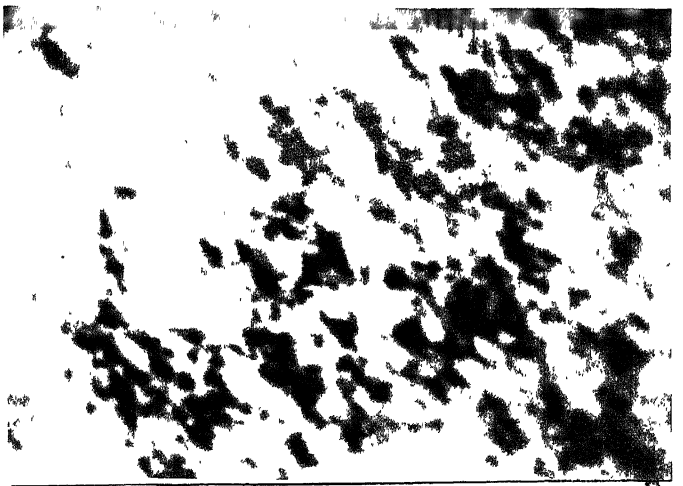

Fig.4.31: Annealed and aged at 350°C for 10 minutes - Mag. 190,000X.

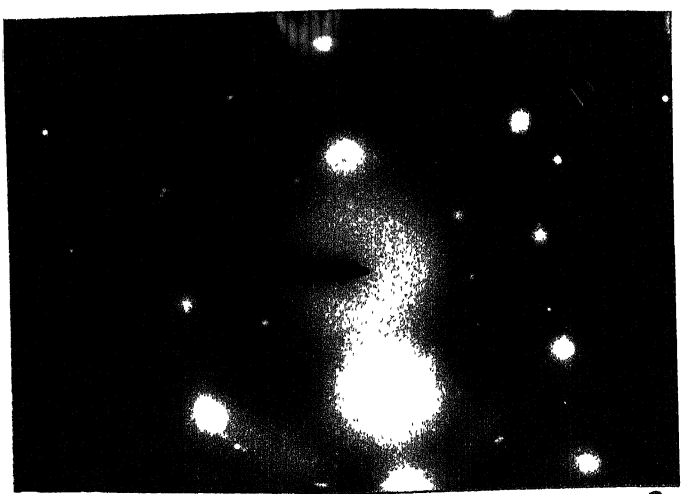

Fig.4.32: Annealed and aged at 350°C for 10 minutes

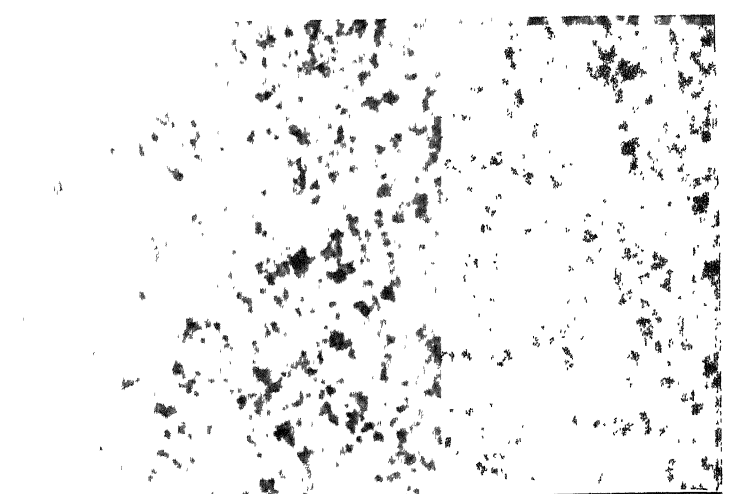

Fig.4.33: Annealed and aged at 350°C for 30 minutes - Mag.190,000X.

Fig. 4.34: Annealed and aged at 350°C for 30 minutes

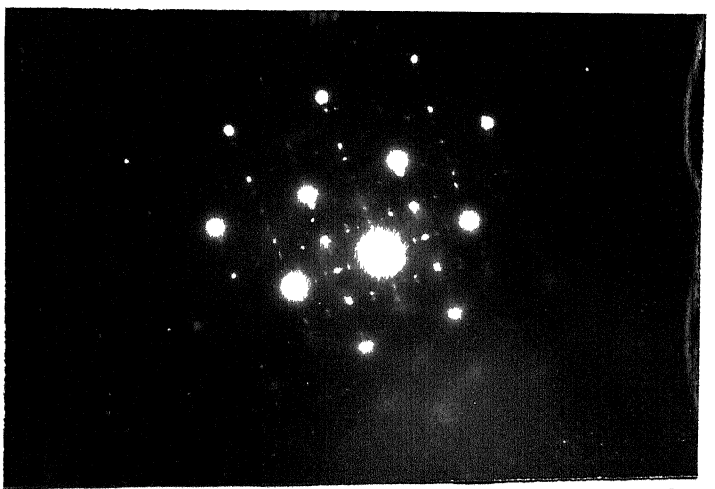

Fig. 4.35: Annealed and aged at 350°C for 30 minutes

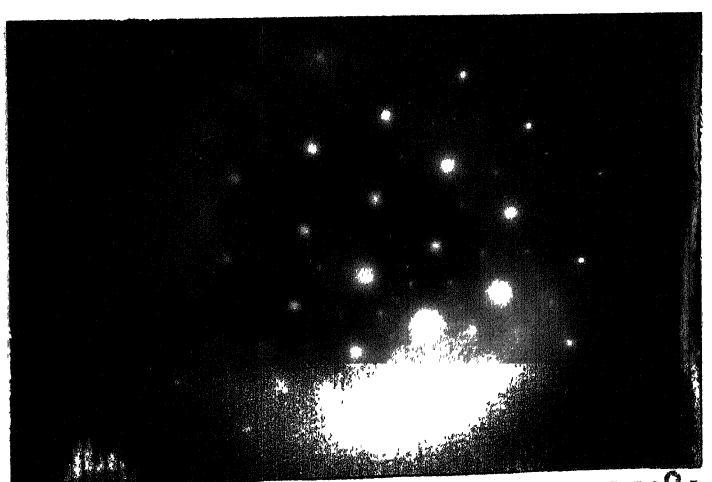

Fig. 4.36: Annealed and aged at 350°C for 30 minutes

is the presence of a well defined precipitate free zone on both sides of the grain boundary. Figure 4.40 shows the micrograph of the alloy aged for 5 hours. A group of lamellar discontinuous precipitates can be seen in the matrix. The lamellae in any one group are nearly parallel to one another. The corresponding SAD is shown in Figure 4.41. The micrograph of the alloy aged for 10 hours is shown in Figure 4.42. The discontinuous precipitates which were observed before are in a more advanced stage of growth. The average interlammelar spacing as well as the average width of the lamellae are found to have increased. In addition some other precipitates can also be seen in the interlamellar space. The corresponding SAD is shown in Figure 4.43. The micrograph of the alloy aged for 20 hours is shown in Figure 4.44. A few colonies of lamellar precipitates can be seen at this stage. The average width of the lamellae, the interlamellar spacing and the morphology of the lamellae varies widely from one colony to another. Figure 4.45 is the micrograph of the alloy that has been aged for 100 hours. The lamellar nature of the discontinuous precipitates is retained even after such prolonged aging. The corresponding SADis shown in Figure 4.46.

4.4 <u>SEM Results</u>:

Figure 4.47 is the micrograph of the 95 per cent cold worked alloy. The fracture surface shows a mixture of

Fig. 4.40: Annealed and aged at 350°C for 5 Hours - Mag.51,000X.

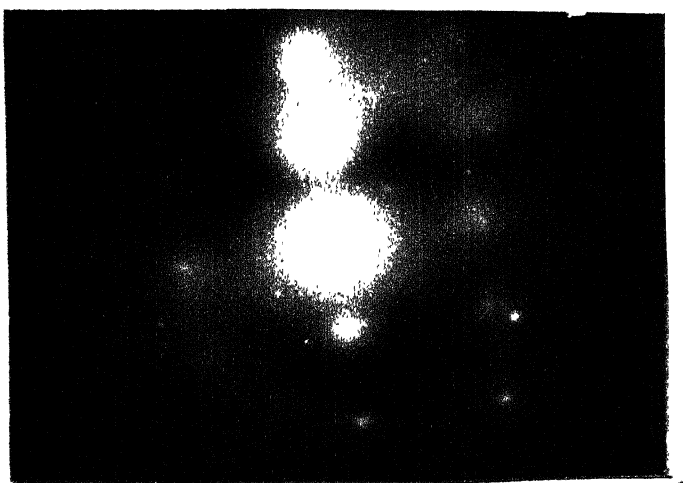

Fig. 4.41: Annealed and aged at 350° for 5 Hours

Fig. 4.42: Annealed and aged at 350°C for 10 hours - Mag.39,000X.

Fig. 4.43: Annealed and aged at 350°C for 10 hours

Fig. 4.44: Annealed and aged at 350°C for 20 hours -Mag.39,000X.

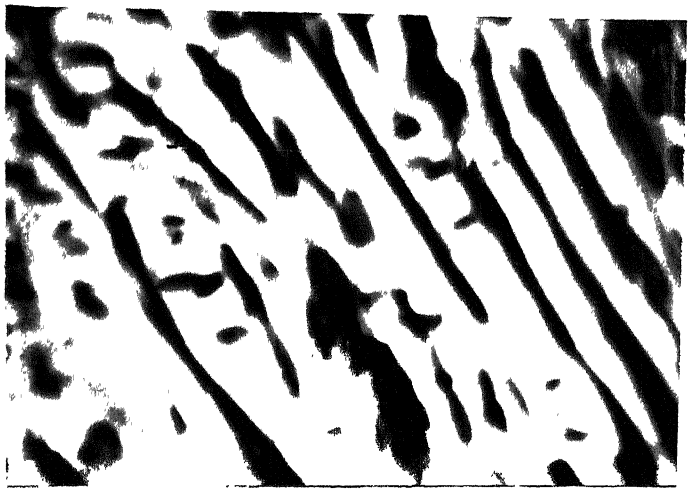

Fig. 4.45: Annealed and aged at 350°C for 100 hours - Mag.51,000X.

Fig. 4.46: Annealed and aged at 350°C for 100 hours

the brittle type and ductile type. Both the cleavage [illegible] and dimples are visible. Figure 4.48 shows a magnified image of the cleavage phase for the cold worked alloy. The presence of a few ridges can be clearly seen. The fracture surface does not change much on aging the cold worked alloy at 550°C upto 2 minutes (Figures 4.49 and 4.50). Figures 4.51 and 4.52 are the micrograph of the alloy aged at 550°C for 10 and 20 minutes respectively after cold rolling. The fracture surface does not show any dimple like feature in these cases. However, the fracture does not look like a purely brittle type either.

4.5 Results of X-Ray Diffraction:

The results of x-ray diffraction made on a number of samples at various conditions are given in a tabular form in Table 4.1. The details showing the d-value of the lines observed with their relative intensities for each sample are given in Appendix I.

4.6 Differential Thermal Analysis (DTA) Results:

The results of the DTA carried out on the annealed alloy are shown in Figure 4.53.

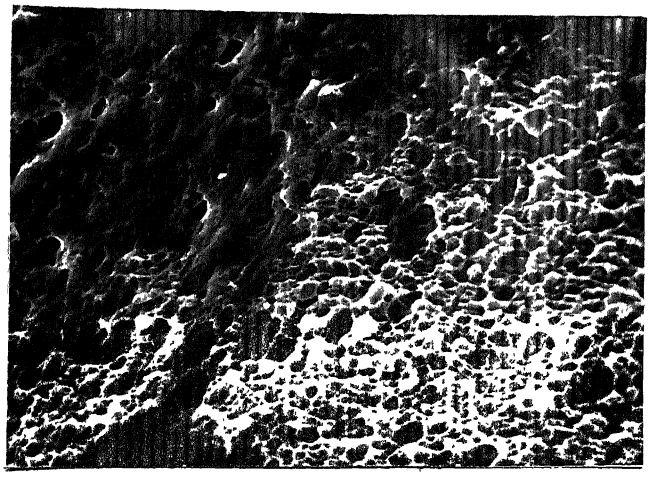

Fig. 4.47: Cold rolled - Mag. 800X.

Fig. 4.48: Cold rolled - Mag. 400X.

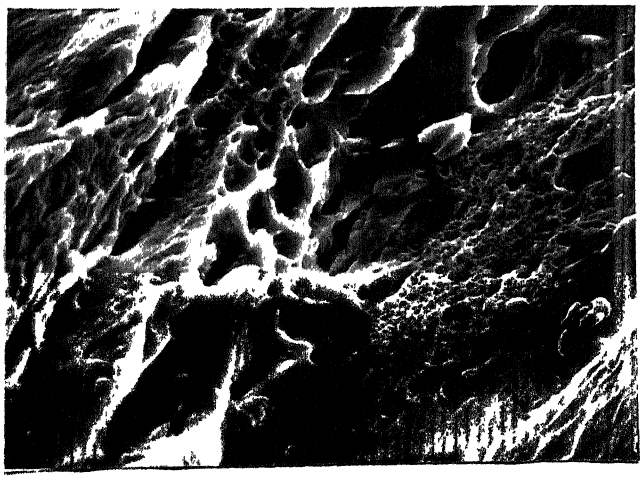

Fig. 4.49: Cold rolled and aged at 350°C

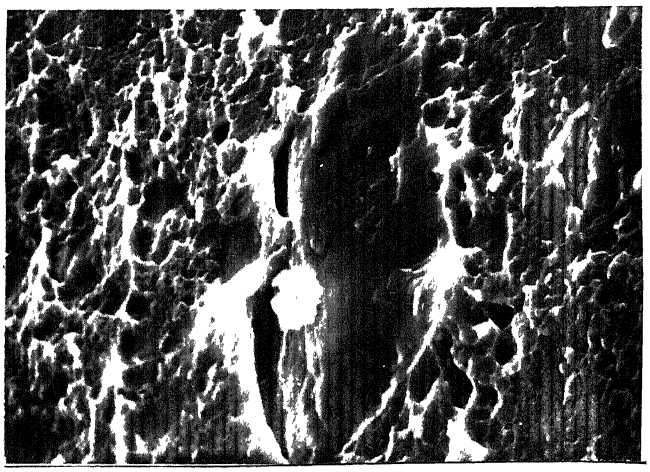

Fig. 4.50: Cold rolled and aged at 350°C for 2 minutes - Mag. 1600X.

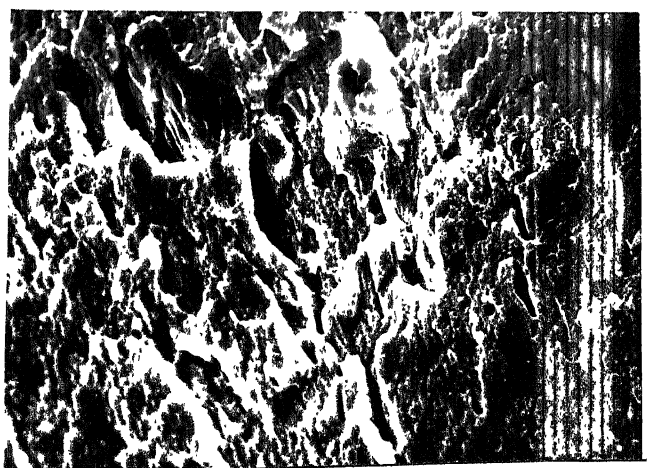

Fig. 4.51: Cold rolled and aged at 350°C for 10 minutes - Mag. 800X.

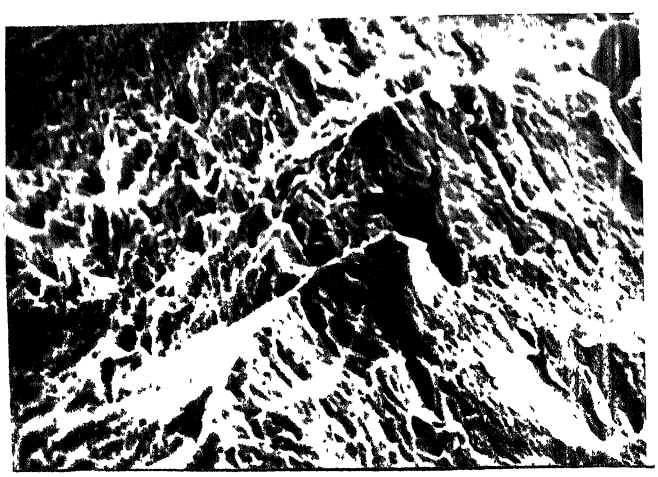

Fig. 4.52: Cold rolled and aged at 350°C For 20 minutes - Mag. 800X.

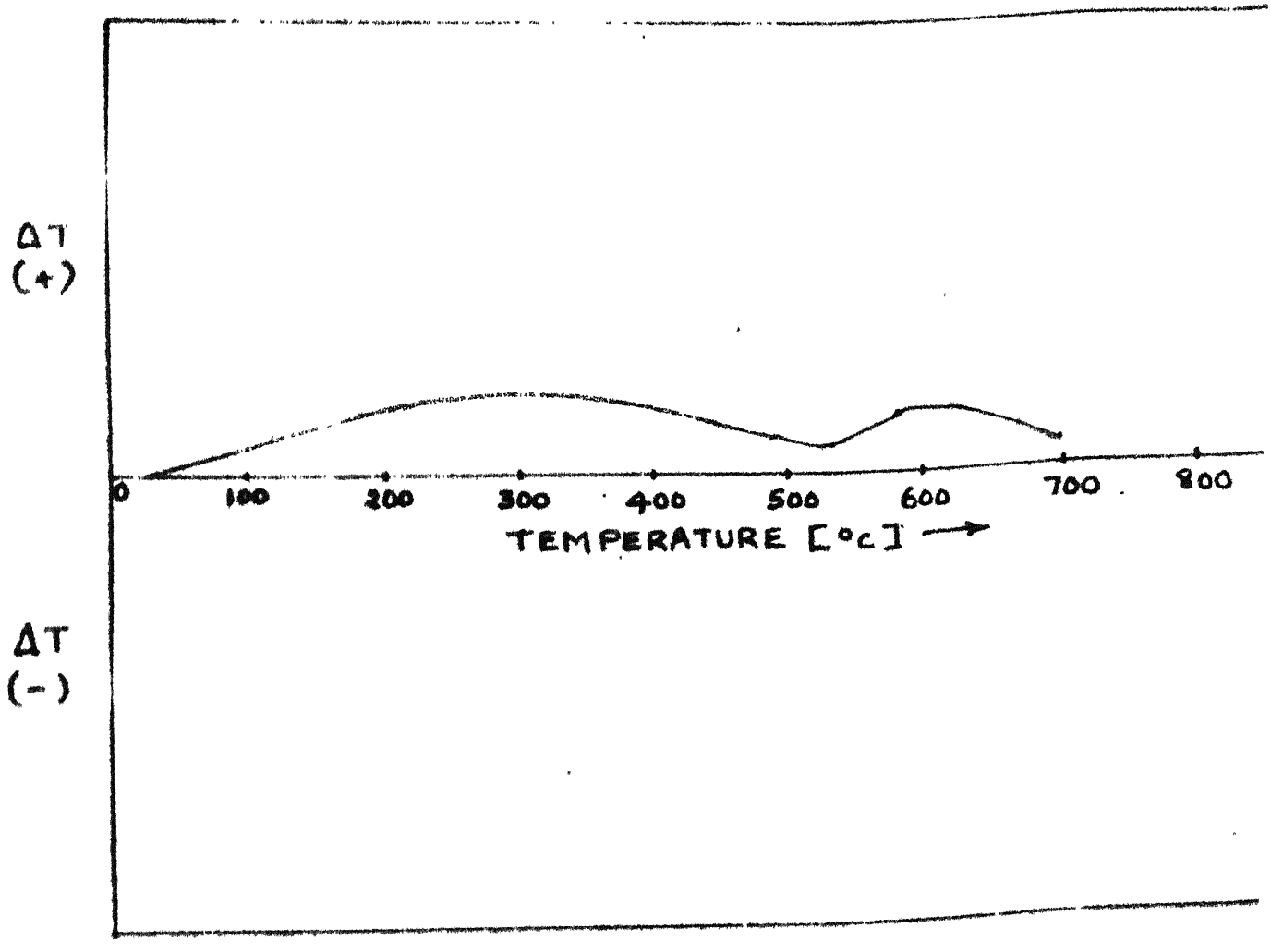

Fig. 4.53 - D.T.A. curve for annealed Cu-9Ni-6Sn alloy.

TABLE 4.4: RESULTS OF X-RAY STUDY

Condition of the Alloy	Phase/Phases identified
Annealed at 825°C	α-solid solution
Annealed at 825°C and aged at 350°C for 30 mins.	α-solid solution + x
Annealed at 825°C and aged at 350°C for 1 hour	α-solid solution + x
Annealed at 825°C and aged at 350°C for 5 hours	α-solid solution + $(CuNi)_3Sn$ + x
Annealed at 825°C and aged at 350°C for 20 hours	α-solid solution + $(CuNi)_3Sn$ + x
Cold worked and aged at 350°C for 20 hours	α-solid solution + $(CuNi)_3Sn$ + x

x- A number of lines could not be identified.

CHAPTER 5

DISCUSSION OF RESULTS

Extensive electron microscopy of the present alloy in the prior cold-worked/aged and non prior cold-worked/aged conditions clearly indicate three distinct stages of pre-precipitation/precipitation consequent upon aging. The most significant point to note is that the sequence of the changes occurring in this alloy on aging is not altered depending on whether the alloy is prior cold-worked or not. The only difference that is noticed between these two conditions is that in the prior cold-worked material these stages are somewhat shifted to a higher aging temperature.

Broadly speaking, on aging, the present alloy shows the following three phenomena in sequence:

(i) Formation of a spinodal decomposition product

(ii) Formation of an ordered phase

(iii) Discontinuous precipitation at a later stage.

Of course, in case of the prior cold-worked material, on aging, recovery and recrystallisation of the highly dislocated matrix take place along with the precipitation processes.

As has been stated earlier the material annealed at 825°C and quenched is an F.C.C. solid solution of Ni and In atoms in the copper matrix. Electron microstructure at

this stage shows hardly any features excepting almost dislocation free grains. Things do not change much till the material is aged at 350°C for 10 minutes (Figure 4.31). A modulated structure can be clearly seen at this stage indicating that spinodal decomposition has taken place. The wavelength of the modulations is approximately 50 Å. The 200 matrix spot in the corresponding diffraction pattern(Figure 4.32) is unusually big and smeared which may be due to the very close proximity of satellite spots flanking the matrix spot. Evidently the spinodal decomposition progresses with aging time and after 30 minutes the modulations become more pronounced (Figure 4.33). However, at this stage together with the modulated structure some fine precipitates can also be seen. In fact SAD taken from two such regions with precipitates (Figures 4.35 and 4.36) show clearly the formation of an ordered phase. In these photographs superlattice spots forming different types of patterns can be clearly seen along with the matrix spots. Although the crystallography and other details about this ordered phase has not yet been determined, attempts are underway to do so. The formation of the ordered phase could be detected after 1 hour aging at 350°C. However, after aging the material for 2 hours at 350°C things started changing drastically. At this stage a discontinuous precipitate could be seen present both at the grain boundaries as well as

grain interiors. Clearly formed denuded zones around grain boundaries (Figure 4.39) can also be seen at this stage. With the progress of aging at 350°C the discontinuous precipitates could be found to assume a lamellar shape.

The D.T.A. curve for the annealed alloy (Figure 4.53) shows two clear-cut humps - the peaks appearing at around 300°C and 600°C. As the experimental results clearly indicate it is extremely difficult to find out where the spinodal decomposition ends and the formation of the ordered precipitates takes place. It may be postulated that due to the spinodal decomposition a composition fluctuation occurs throughout the matrix thus creating alternate solute-depleted and solute-rich zones. It is likely that ordering takes place in the solute-rich regions ultimately producing the ordered precipitates. Eventually, discontinuous precipitates formed at specific regions grow and engulf the whole of the matrix. It is suggested that the first hump in the D.T.A. curve may be associated with the spinodal decomposition and formation of ordered precipitates whereas the second hump may be associated with the formation of the discontinuous precipitation phase.

As mentioned earlier, in the cold-worked alloy heat-treated at 350°C for various lengths of time the sequence of the above reactions is maintained but shifted to higher aging time. Thus it may be seen that fine striation-like

modulations are present in the microstructures of aged prior cold worked samples also (Figures 4.14, 4.15, 4.17, 4.19). The wavelength of the modulations lie within the range 50-100 Å. The ordered precipitates in this case appear at a much later stage, viz. after 20 hours of aging at 350°C (Figures 4.21 and 4.22). Finally the discontinuous precipitates form and engulf the entire region. Side by side with precipitation, the alloy recovers and finally recrystallises with progressive aging.

A number of partly and fully recrystallised microstructures can be seen in Figures 4.26 to 4.29. These all correspond to the alloy which has been cold-worked and then aged at 600°C for various lengths of time. The important point to note here is that the discontinuous precipitate seems to form quite early during the aging process both in the cold-worked and the recrystallised regions. Because of the much higher aging temperature recrystallisation is much faster here.

Spinodal decomposition in non-prior cold-worked and aged Cu-Ni-Sn alloys have been reported by a few workers [2, 16]. Spinodal decomposition in prior cold-worked and aged Cu-Ni-Sn and Cu-Ti alloys have also been reported by a few authors [2,13]. However, Helmi and Zsoldos [3] have put forward some evidence to show that the heavily deformed state of the lattice prevents spinodal decomposition of the

copper-rich Cu-Ni-Sn systems. The results of the present investigation, however, support the views of Plewes [2] and Dutkiewicz [13] and are contrary to those of Helmi and Zsoldos [3].

The formation of the ordered phase during the aging process of non-prior cold-worked Cu-Ni-Sn alloy has been reported by Baburaj et al.[16]. No other worker working on the same system has shown any evidence of the deformation of the ordered phase. The present investigation shows that the ordered phase forms not only during aging of the non-prior cold worked material but also during the aging of the prior heavily deformed material.

The mechanical property values like Y.S., U.T.S. and P.E. in this alloy at any condition may be directly correlated to the corresponding microstructures. For example, for the non prior cold-worked material which is given the aging treatment the maximum value of Y.S.(86.9 Ksi) and U.T.S.(99.5 Ksi) are found to be attained when the microstructure shows a highly modulated structure. Formation of the ordered precipitate does not seem to have much significant effect on these values which however seem to come down drastically with the formation of the discontinuous lamellar precipitation. The percentage elongation value also comes down to the minimum when the lamellar precipitation is fully developed.

Precisely similar trend is noticed with the mechanical property values of the prior cold-worked and low temperature (350°C) aged material. The maxima in Y.S. and U.T.S. are obtained when the structure is fully modulated. The reason why the mechanical property values are about two orders of magnitude higher in the prior cold-worked and aged material with respect to its non-prior cold-worked counterpart is the extra hardening imparted by the highly dislocated matrix to the otherwise modulated matrix as a result of the spinodal decomposition. In fact an optimum combination of all the mechanical property values may be achieved by choosing the proper amount of cold deformation together with the proper heat-treatment.

The mechanical property values of the alloy prior cold-worked and aged at 600°C are, in general, much lower compared to the corresponding values for the alloy heat-treated at a lower temperature of 350°C. This may be explained as due to much faster recrystallisation in the former compared to the latter.

CHAPTER 6

CONCLUSION

1. The Cu-9Ni-6Sn alloy is highly age-hardenable and shows a number of phase transitions on aging.

2. The transformation sequence in both the prior cold-worked and aged as well as non prior cold-worked and aged alloy has been found to be: Solid solution ---- Spinodal decomposition -- Ordered precipitation - Discontinuous precipitation.

3. The successive phase transitions have been found to be more sluggish and occur over longer periods of aging time in case of the prior cold worked material.

4. The discontinuous grain-boundary precipitation on aging is almost totally suppressed in the prior cold-worked alloy.

5. Thermomechanical treatment has been found to be very effective in improving the mechanical properties of this alloy. Optimum mechanical properties (in respect of yield strength and tensile strength) have been obtained on cold rolling to 95 per cent reduction followed by aging at 350°C for 10 minutes.

6. The high strength achieved by TMT in this alloy is supposed to be due to the combination of two factors -

the stabilised high dislocation density in the cold-worked material and the presence of a modulated structure produced by spinodal decomposition.

REFERENCES

1. R.R. Hart, B.C.Wonsiewicz and G.Y.Chin: Met. Trans., 1970, Vol.1, p.3163.
2. J.T. Plewes: Met.Trans., 1975, Vol.6A, p.537.
3. F.M. Hobbi and L.Zsoldos: Scripta Met., 1977, Vol.11, p.899.
4. Materials Engineering, 1977, Vol.86, No.6, p.93.
5. M.J. Saarivirta and H.S. Cannon: Metal Progress, 1959, Vol.76, p.81.
6. W. Leo: Metall., 1957, Vol.21, p.908.
7. L.H. Schwartz, S. Mahajan and J.T. Plewes: Acta Met., 1974, Vol.22, p.601.
8. L.E. Tanner: Phil. Mag., 1966, Vol.14, p.111.
9. G. Thomas: Electron Microscopy and Strength of Crystals, p.793, John Wiley and Sons, 1963.
10. S. Yamamoto, M.Matsui and Y. Murakami: Trans. J.I.M., 1971, Vol. 12, p.119.
11. J.A. Cornie, A.Datta and W.A. Soffa: Met. Trans., Vol. 4A, 1973, p.727.
12. V.Daniel and H. Lipson: Proc. Roy.Soc., 1944, Vol.A182, p.310.
13. J. Dutkiewicz: Met.Trans., Vol.8A, 1977, p.751.
14. A. Datta and W.A. Soffa: Acta Met. 1976, Vol.24, p.987.
15. D.E. Laughlin and J.W. Cahn: Acta Met. 1975, Vol. 23, p.329.

16. E.G. Baburaj, U.D. Kulkarni, E.S.K. Menon, and R. Krishnan: J. Appl. Cryst., 1979, 12 (to be published).

17. A.L. Wingrove: J. Inst. Metals, 1972, Vol.100, p.313.

18. W.G. Truckner and D.E. Mikkola, Met. Trans. 1977, Vol.8A, p.45.

19. T.C. Tisone, G.Y. Chin and B.C. Wonsiewicz: Met. Trans., 1970, Vol.1, p.2010.

20. R.N. Caron and S. Shapiro: Met. Trans., 1977, Vol.8A, p.111.

21. J.W. Cahn: Trans. T.M.S.AIME, 1968, Vol.242, p.166.

22. J.W. Cahn: Acta Met., 1961, Vol.9, p.795.

23. J.W. Cahn: Acta Met., 1962, Vol. 10, p. 179.

24. A.J. Bradley: Proc. Phys.Soc., 1940, Vol.52, p.80.

25. E.P. Butler and G. Thomas: Acta Met., 1970, Vol. 18, p.347.

26. B.G. Lefevre, A.T. D'Annesa and D. Kalish: Met. Trans. 1978, Vol. 9A, p.577.

27. J.W. Cahn: Acta Met., 1963, Vol. 11, p.1275.

28. P.M. Ghista and W.D. Nix, Mat. Sci. Engg., 1969, Vol.3, p.293.

29. N.F. Mott and F.R.N. Nabarro: Proc. Phys. Soc. 1946, Vol. 58, p.669.

30. J.R. Mihalson, E. Huston and F.A. Badia: Trans. ASM., 1967, Vol.60, p.395.

31. E. Orowan: Symposium on internal stresses in Metals and Alloys, p.451, Institute of Metals, 1948.

32. A. Kelly and M.E. Fine: Acta Met., 1957, Vol.5, p.365.

APPENDIX

Annealed at 825°C

d	Relative intensity
2.0930	Strong
2.0046	Moderately strong
1.8136	Very strong
1.2830	Strong

Annealed at 825°C and Aged at 350°C for 30 Mins.

d	Relative intensity
2.3082	Weak
2.1007	Very strong
1.8164	Very strong
1.4137	Very weak
1.2818	Strong
1.2084	Moderately strong

Annealed at 825°C and Aged at 350°C for 1 Hour:

d	Relative intensity
2.3082	Moderately strong
2.0930	Very strong
1.8164	Very strong
1.2830	Strong
2.4623	Weak
2.1820	Very weak
2.0116	Very weak

Annealed at 825°C and Aged at 350°C for 5 Hours:

d	Relative intensity
2.3082	Moderately strong
2.0814	Very strong
1.8164	Strong
1.4137	Moderately strong
1.2830	Strong
1.4743	Very weak
2.6469	Very weak
2.4790	Very weak

Annealed at 825°C and Aged at 350°C for 20 hours:

d	Relative Intensity
3.3237	Very weak
2.5060	Very weak
2.3075	Strong
2.0896	Very strong
1.9959	Strong
1.8790	Very weak
1.7990	Very weak
1.4104	Weak
1.3329	Very weak
1.2754	Very strong
1.2046	Weak
1.0893	Very strong
1.0427	Strong

Cold-worked and Aged at 350°C for 20 Hours:

d	Relative intensity
2.4623	Weak
2.2986	Weak
2.0814	Very strong
1.8053	Strong
1.4107	Strong
1.2761	Very strong
1.2093	Weak
1.4828	Very weak

A 62176

Date Slip

ıe This book is to be returned on the date last stamped.

....	.....	.....
....	.....	.....
....	.....	.....
....	.....	.....
....	.....	.....
....	.....	.....
....	.....	.....
....	.....	.....
....	.....	.....
....	.....	.....
....	.....	.....

CD 6.72.9

ME - 1979 - M - DEV - STR